Synthesis of linear chitosan-block-dextran copolysaccharides with dihydrazide and dioxyamine linkers

Elise Courtecuisse, Sylvain Bourasseau, Bjørn E. Christensen, Christophe Schatz

Author manuscript version of *Carbohydrate Polymers*, 2024, 345, 122576 DOI: 10.1016/j.carbpol.2024.122576

Synthesis of linear chitosan-*block*-dextran copolysaccharides with dihydrazide and dioxyamine linkers

Elise Courtecuisse[a], Sylvain Bourasseau[a], Bjørn E. Christensen[b,*], Christophe Schatz[a,*]

[a] Université de Bordeaux, CNRS, Bordeaux INP, Laboratoire de chimie des polymères organiques (LCPO), UMR 5629, 33600 Pessac, France

[b] NOBIPOL - Department of Biotechnology and Food Science, NTNU, Trondheim, Norway

[*] Corresponding authors

E-mail addresses: bjorn.e.christensen@ntnu.no (B.E. Christensen), schatz@enscbp.fr (C. Schatz).

Abstract

Dihydrazide (ADH) and dioxyamine (PDHA) were assessed for their efficacy in coupling chitosan and dextran via their reducing ends. Initially, the end-functionalization of the individual polysaccharide blocks was investigated. Under non-reducing conditions, chitosan with a 2,5-anhydro-D-mannose unit at its reducing end exhibited high reactivity with both PDHA and ADH. Dextran, with a normal reducing end, showed superior reactivity with PDHA compared to ADH, although complete conversion with ADH could be achieved under reductive conditions with $NaBH_3CN$. Importantly, the oxime bond in PDHA conjugates exhibited greater stability against hydrolysis compared to the hydrazone bond in ADH conjugates. The optimal block coupling method consisted in reacting chitosan with an excess of dextran pre-functionalized with PDHA. The copolysaccharides could be synthesized in high yields under both reducing and non-reducing conditions. This methodology was applied to relatively long polysaccharide blocks with molecular weight up to 14,000 g/mol for chitosan and up to 40,000 g/mol for dextran. Surprisingly, block copolysaccharides did not self-assemble at neutral or basic pH; rather, they precipitated due to hydrogen bonding between neutralized amino groups of chitosan. However, nanoparticles could be obtained through a nanoprecipitation approach.

Key words: chitosan; dextran; hydrazone; oxime; conjugate; block copolymer

1. Introduction

Chitosan and dextran are two polysaccharides commonly used for biomedical applications (Dumitriu, 2004). Chitosan, a biopolymer derived from chitin, is composed of 2-amino-2-deoxy-D-glucan (GlcN) and 2-acetamido-2-deoxy-D-glucan (GlcNAc) units linked by β-(1→4) bonds. Chitosan is known for its biocompatibility, biodegradability, and antimicrobial properties. It has been widely employed in drug and gene delivery systems, wound healing, tissue engineering, and as a coating for biomedical implants. Chitosan, behaves in aqueous solution as a weak polybase with a value of intrinsic pK_a (pK_0) varying from 6.5 to 7.3, depending on the degree of acetylation (DA) (Sorlier et al., 2001). As such, chitosan has good complexing properties with negatively charged polymers, particles, and surfaces at pH below 6. Dextran, on the other hand, is a PEG-like neutral polymer with excellent water solubility and low toxicity. It is a linear polymer composed of D-glucose units linked by α-(1→6) bonds, with a small number of side chains consisting of 1 or 2 D-glucose units mainly linked by α-(1→3) bonds to the backbone units. Dextran is often utilized as a drug carrier, in imaging applications, and as a plasma expander due to its ability to increase blood volume. The two polysaccharides have different chain conformation. Dextran has an extendable coil conformation due to its flexible α-(1→6) glycosidic linkages. However, it has been reported that in the low molar mass ranges (M < 2,000 g/mol), dextran oligosaccharides adopt a rodlike conformation (Gekko, 1981). On contrary, chitosan is a relatively stiff molecule due to the diequatorial glycosidic bonds in the $^4C_1$ ring conformation, which restrict rotation, and the electrostatic repulsions between charged units. Persistence lengths of 0.4-1.8 nm and 5-9 nm

have been reported for dextran (Rief et al., 1998; White & Deen, 2002) and chitosan (Berth et al., 1998; Schatz et al., 2003; Weinhold & Thöming, 2011), respectively.

In this work we propose to synthesize rod-coil block copolymers from chitosan and dextran in order to combine the properties of the two polysaccharide blocks within a single polymer chain. As a consequence, we will refer to them as block copolysaccharides. Linear block copolymer structures are specifically targeted to preserve the intrinsic properties of each block (Schatz & Lecommandoux, 2010; Volokhova et al., 2020). The difficulty in synthesizing linear block copolysaccharides lies in the low abundance of the reactive aldehyde form of the reducing end, which is in equilibrium with its cyclic hemiacetal form (Dworkin & Miller, 2000; Los et al., 1956). Amination is an effective approach to modify the reducing end and thus functionalize the chain end of polysaccharides. However, due to the low availability of aldehyde groups, the amination rate is relatively low. By stabilizing the imine intermediate through reduction, the reaction is driven forward, increasing the overall yield of the amination process. A common reducing agent is sodium cyanoborohydride ($NaBH_3CN$), which is milder than sodium borohydride ($NaBH_4$) and selective for the reduction of imines over aldehydes or ketones. Since the reduction rate of iminium ions with $NaBH_3CN$ is faster than for aldehydes, the amination can be carried out using a one-pot approach in which the reducing agent is introduced at the beginning of the reaction (Borch et al., 1971). This approach, known as reductive amination, is effective for conjugating small ligands to the reducing ends of polysaccharides but is less effective for long polymer blocks due to the low probability of the chain ends encountering (Bosker et al., 2003). In this regard, azide-alkyne click chemistry (Breitenbach et al., 2017) and oxime formation (Novoa-Carballal & Müller, 2012) have been shown to be more effective for the synthesis of polysaccharide-containing copolymers.

We have recently introduced dihydrazide and dioxyamine agents as powerful linkers for coupling the reducing end of various oligosaccharides, including chitin, chitosan, dextran and oligoguluronate (Coudurier et al., 2020; Mo et al., 2020; Moussa et al., 2019; Solberg et al., 2021, 2022; Vikøren Mo et al., 2020). The linkers are adipic acid dihydrazide (ADH) and O,O′-1,3-propanediylbishydroxylamine (PDHA), which are both commercially available. The coupling reactions were conducted under non-reductive conditions, resulting in the formation of hydrazone and oxime bonds, or in the presence of a reducing agent such as $NaBH_3CN$ or picoline borane to produce stable secondary amines. The high reactivity of hydrazide and oxyamine with reducing carbohydrates contrasts with that of most primary amines (Baudendistel et al., 2016; Khadem & Fatiadi, 2000; Kölmel & Kool, 2017; Kwase et al., 2013). This is due to the stronger nucleophilicity of oxyamine and hydrazide groups which arises from the "alpha effect" – an increase in the energy of the Highest Occupied Molecular Orbital (HOMO) due to the orbital overlap of neighboring (alpha) atoms having lone electron pairs (Edwards & Pearson, 1962; Hansen et al., 2021). Furthermore, the low basicity of hydrazide and oxyamine (pK_a between 3 and 4) contributes to the formation of more stable imine products under acidic conditions (Kalia & Raines, 2008). This is particularly important for chitosan, which is only soluble in slightly acid conditions. In contrast to the three-step azide-alkyne click chemistry, which involves the end-functionalization of each polysaccharide block, block coupling using ADH/PDHA linkers can be achieved in just two steps (Scheme 1). Moreover, this approach eliminates the need for a copper catalyst, which could potentially interact with certain polysaccharides.

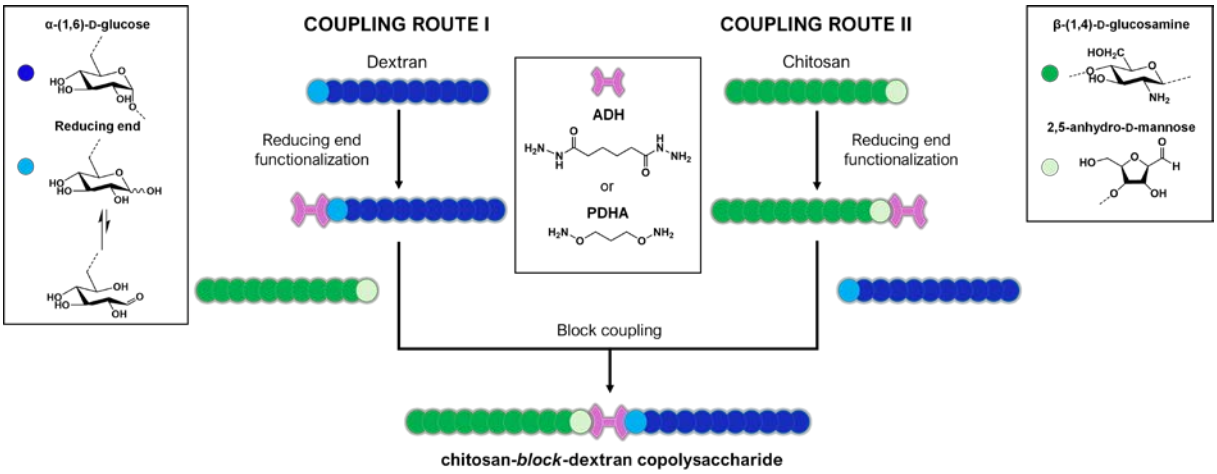

Scheme 1. Two-step synthesis of chitosan-*block*-dextran copolysaccharides using dihydrazide (ADH) and dioxyamine (PDHA) linkers.

In previous studies, we primarily focused on terminal functionalization of chitin oligomers with ADH/PDHA and subsequent coupling reactions with oligosaccharides like dextran of low degrees of polymerization (DP ≤ 5), which were fractionated by gel filtration chromatography (Mo et al., 2020; Vikøren Mo et al., 2020). This allowed for a detailed characterization of the conjugates using NMR spectroscopy. The aim of the present study is to extend the research to longer polysaccharides, using chitosan and dextran of relatively high DPs. The objective is to define the optimal synthesis pathway for chitosan-*block*-dextran copolysaccharides in terms of yield and purity, which could potentially be applied to any polysaccharide blocks in the future. At first, we aim to identify the most suitable linker for coupling, choosing between ADH and PDHA. To achieve this, we examined the modification of the reducing end of the two polysaccharide blocks with ADH and PDHA, both with and without reducing agent. Next, we aim to determine which polysaccharide block should be preferentially pre-functionalized with the linker before reacting it with the native polysaccharide block. This implies to investigate each of the four possible coupling routes individually, as depicted in Scheme 1. By doing so, some unexpected side-reactions were highlighted. Lastly, we aim at applying the most effective route to the coupling of chitosan and dextran with relatively large molecular weights - up to 14,000 g/mol for chitosan and 40,000 g/mol for dextran. Following purification, the solubility properties of the block copolysaccharides were assessed at different pHs, as well as their ability to form nanoparticles under specific conditions.

As double-hydrophilic block copolymers, chitosan-*block*-dextran copolymers are well suited to form polyion complex micelles with charged biomolecules such as nucleic acids or proteins. Therefore, they can be used as delivery systems for various biological purposes. Additionally, they can be utilized for decorating negatively charged surfaces and colloids through a simple adsorption process. These applications leverage the complexing properties of chitosan and the anti-fouling properties and associated stealth effect of dextran.

2. Experimental section

2.1. Materials

Chitosan (41 kg/mol, degree of acetylation (DA) of 4%) was obtained from Stellar Biosol (Gujarat, India, chitosan batch 144/090605) (Figure S1). Dextrans of various molar masses (5, 10, 20 kg/mol) were purchased from Pharmacosmos. Dextran of 40 kg/mol was purchased from Fluka. Adipic acid dihydrazide (ADH), O,O'-1,3-propanediylbishydroxylamine dihydrochloride (PDHA) and sodium cyanoborohydride ($NaBH_3CN$) were obtained from Sigma-Aldrich. All other chemicals were obtained from commercial sources and were of analytical grade.

2.2. Chitosan depolymerization

The starting chitosan was depolymerized with sodium nitrite ($NaNO_2$) into chitosan of different degrees of polymerization (DP) according to previously reported protocols with some variations (Chapelle et al., 2019; Coudurier et al., 2020; Delas et al., 2019; Mo et al., 2020; Tømmeraas et al., 2001). In brief, chitosan (41 kg/mol, DA 4%) was dissolved at a concentration of 2.5 g/L in milli-Q water with the stoichiometric amount of HCl relative to amine functions. An excess of 10% was added to ensure full protonation of glucosamine residues. The solution was left under stirring overnight. Various amounts of $NaNO_2$ were added so that the [GlcN]/[$NaNO_2$] molar ratio varied from 7 to 57 (Supporting Information S2). The reaction was allowed to proceed overnight at room temperature. The solution was filtered on 1 µm pore size glass fiber membrane to remove insoluble polymer particles. Then, chitosan was precipitated by addition of 1 volume of MeOH:NH_3 (1:1) mixture to 2.5 volumes of chitosan solution. Subsequently, the medium was centrifuged (15 min, 6,000 x g) at room temperature and the pellets were washed with water and centrifuged several more times until the pH of the supernatant was neutral. At this stage some chitosan fractions of low DP (< 20) may have been lost due to their water-solubility at neutral pH (Chapelle et al., 2019). Depolymerized chitosan was finally recovered by freeze-drying. The values of DP used below always include the terminal 2,5-anhydro-D-mannose unit (M-unit).

2.3. Dextran end-functionalization with ADH and PDHA

Dextran was dissolved at a concentration of 60 g/L in 500 mM acetate buffer pH 4.0 for at least 2 hours with stirring at room temperature. 20 equivalents of ADH or PDHA relative to the mole number of reducing end in dextran were dissolved in a minimum amount of buffer. The pH was adjusted to 4.0 if needed. ADH or PDHA was then added to the dextran solution and the reaction was left under stirring for 12 hours at room temperature. For the reduction step, if required, 10 eq. of sodium cyanoborohydride ($NaBH_3CN$), were dissolved in a minimum amount of buffer and added to the dextran/ADH solution. The reaction was left under stirring overnight at room temperature. For dextran/PDHA, 2 x 10 eq. additional $NaBH_3CN$ were added at intervals of 12 hours. The end-functionalized dextrans, reduced or not, were precipitated with 20-fold excess of technical grade ethanol at room temperature. The solutions were centrifuged (15 min, 6,000 x g) at room temperature. The supernatants were discarded and the pellets dried under dynamic vacuum during 4 hours at room temperature. The pellets were then dissolved in milli-Q water and ultrafiltered with 3 x 300 mL of water using a Amicon stirred cell with a cellulose membrane having a molecular weight cut-off (MWCO) of 1 kDa. Finally, the end-functionalized dextrans were recovered by freeze-drying.

2.4. Chitosan end-functionalization with ADH and PDHA

Chitosan was dissolved under stirring overnight at a concentration of 20 g/L in milli-Q water with the stoichiometric amount of HCl relative to amine functions. The pH was then adjusted to 4.0. 20 equivalents of ADH or PDHA, relative to the mole number of reducing end of chitosan, were dissolved in a minimum amount of water. The pH was adjusted to 4.0, if needed, before addition to the chitosan solution. The reaction was left under stirring for 12 hours at room temperature. For the reduction step, if required, 10 eq. of $NaBH_3CN$ dissolved in a minimum of water were added to the chitosan/ADH solution and left stirring overnight at room temperature. For chitosan/PDHA, 3 x 10 eq. additional $NaBH_3CN$ were added at intervals of 12 hours. The functionalized chitosan was precipitated by addition of 1 volume of MeOH:NH_3 (1:1) mixture to 5 volumes of chitosan solution. The medium was centrifuged (15 min, 6,000 x g) at room temperature and the pellets were washed with water and centrifuged again until the pH of the supernatant was neutral. Functionalized chitosan was recovered by freeze-drying.

2.5. Synthesis of linear chitosan-b-dextran block copolysaccharides

Block coupling reactions were performed either by reacting end-functionalized dextran with chitosan or end-functionalized chitosan with dextran. For both methods, chitosan (or chitosan-ADH/PDHA) was dissolved under stirring overnight at a concentration of 20 g/L in milli-Q water with the stoichiometric

amount of HCl relative to amine functions. The pH of the solution was adjusted to 4.0. Then, three equivalents of dextran-ADH/PDHA (or dextran) were dissolved in water with the pH also adjusted to 4.0 before being added to the chitosan solution and left stirring for 12 hours at room temperature. For the reduction step, if required, 10 eq. of $NaBH_3CN$ were dissolved in a minimum amount of water and added to the reaction mixture. The reaction was left under stirring overnight at room temperature. For coupling reactions involving PDHA as linker, 5 x 10 eq. additional $NaBH_3CN$ were added at intervals of 24 hours. The copolysaccharides were precipitated by increasing the pH above 10 with 1 M NaOH. The solutions were centrifuged (30 min, 10,000 x g) at room temperature. The supernatant containing excess dextran-ADH/PDHA (or dextran) was discarded and the pellets containing the copolysaccharides were washed once with water and centrifuged again. Multiple washings of the pellets are not recommended to avoid copolymer extraction into the supernatant (Figure S19). The copolysaccharides were then recovered by freeze-drying. For the copolysaccharide obtained from the largest polysaccharide blocks tested in this work ($Chit_{90}$ and $Dext_{152}$) the coupling step was carried in similar conditions but at higher temperature due to the relatively high viscosity of the reaction mixture. Three equivalents of $Dext_{152}$-PDHA in its reduced form were reacted overnight with one equivalent of $Chit_{90}$ at 50°C. Subsequently, the reduction step was performed at room temperature by adding 5 x 10 equivalents of $NaBH_3CN$ at 24-hour intervals.

2.6. Purification of block copolysaccharides

Excess free chitosan was removed form bulk block copolysaccharides by selective precipitation at a defined pH. Copolysaccharides varying in chitosan and dextran composition were dispersed at a concentration of 5 g/L in milli-Q water. The pH was then adjusted to 6.5 ± 0.1. The solutions were left stirring at room temperature for at least 24 hours. The pH was verified and adjusted to 6.5 ± 0.1 if needed. The solutions were centrifuged (30 min, 10,000 x g) at room temperature. The pellets containing mainly free chitosan were discarded. The supernatants were collected and freeze-dried to recover the purified block copolysaccharides.

2.7. Synthesis of dextran-grafted-chitosan copolysaccharides

Chitosan (41 kg/mol, DA 4%) was dissolved under stirring overnight at 5 g/L in acetate buffer (500 mM, pH 4.0). Dextran (10 kg/mol) was added to the chitosan solution and the reaction left under stirring for 2 hours. The number of equivalents of dextran chains relative to amine functions of chitosan was varied from 1:12 to 1:3. Daily additions of 10 eq. of $NaBH_3CN$ were then performed over 15 days. The final solution was dialyzed against water using regenerated cellulose membrane with 3.5 kDa MWCO. The grafted copolysaccharides were recovered by freeze-drying.

2.8. Steric exclusion chromatography (SEC)

SEC measurements were performed at 25°C using an Ultimate 3000 system from ThermoFisher Scientific equipped with a diode array detector (DAD). The system includes a multi-angle light scattering (MALS) detector (HELEOS II, Wyatt) and a differential refractive index detector (Optilab T-rEX, Wyatt). End-functionalized polysaccharides and linear block copolysaccharides were analyzed using TSKgel G3000PWXL and TSKgel G4000PWXL columns (300 mm × 7.8 mm) from TOSOH, covering a molecular weight range from 200 g/mol to 300,000 g/mol. Grafted copolysaccharides were analyzed using TSKgel G5000PWXL and TSKgel G6000PWXL columns (300 mm × 7.8 mm), covering a range from 4 000 g/mol to 8 000 000 g/mol. For the block copolysaccharide purification by SEC, a semi-preparative Shodex OHpak SB-2003 column (300 mm x 20 mm) covering a range from 1,000 to 100,000 g/mol was used and the fractions collected on an Ultimate 3000 fraction collector (experimental conditions reported in supporting information S6). Sodium acetate buffer (0.2 M AcOH/0.15 M AcONa, pH 4.5) was systematically utilized as the eluent at a flow rate of 0.6 mL/min. However, to reduce potential interaction with the stationary phase under acid conditions, dextran-ADH/PDHA conjugates were also analyzed in 0.01 M phosphate buffer at pH 9 + 0.1 M $NaNO_3$ at a flow rate of 0.6 mL/min,

using SHODEX OHpak SB-803 and SB-804 columns (300 mm × 8 mm) covering a molecular weight range from 1 000 g/mol to 400 000 g/mol. All samples were systematically filtered on 0.45 µm pore size cellulose acetate membrane before injection. Chromatograms were acquired with Chromeleon 7.2 software. Data were analyzed with Astra 7.1.0 software. The values of refractive index (dn/dc in mL/g) were determined for each polysaccharide block and copolysaccharide from a range of six concentrations using the Optilab reX refractive index detector. The measurements were performed under the same conditions as for SEC-MALS, with the exception that the buffer was not degassed, and the samples were not filtered prior to analysis.

2.9. Nuclear magnetic resonance (NMR) spectroscopy

Structural characterization of chitosan/dextran conjugates and copolymers was performed by ^{1}H NMR spectroscopy at 298 K on a Bruker AVANCE III HD 400 MHz spectrometer using a 5 mm Bruker multinuclear z-gradient direct probe. The copolymer based on the longest chitosan and dextran blocks was analyzed on a Bruker AVANCE NEO 400 MHz spectrometer (see below). The samples were dissolved at 10 mg/mL in D_2O and adjusted at different pHs using DCl 1.17 M. Since the pH-meter was calibrated with buffers that were not deuterated, the pH meter reading (pH*) was converted to the pD, *i.e*. the real pH, using the formula: pD = pH* + 0.4 (Glasoe & Long, 1960). ^{1}H NMR spectra were calibrated from the signal of HOD at 4.81 ppm. Kinetic studies of dextran and chitosan end-functionalization were performed in deuterated solvents at 298 K on a Bruker AVANCE NEO 400 MHz spectrometer, equipped with a 5 mm BBO Bruker Cryoprobe Prodigy. Dextran was solubilized in 500 mM acetic acid-d_4 and the solution adjusted at pH 4 with NaOD. Chitosan was solubilized in D_2O and the solution adjusted at pH 4 with DCl. The polymer concentration was set to 20 g/L in both cases. The acquisitions were started immediately after the addition of ADH/PDHA in the dextran or chitosan solution in the conditions described above. The reactions were then monitored in the same NMR tube for 24 hours, recording spectra every hour. Data were fitted using a pseudo first order kinetics model as reported previously (Mo et al., 2020; Vikøren Mo et al., 2020). DOSY (Diffusion Ordered Spectroscopy) measurements were performed at 298K on a Bruker Avance III 400 spectrometer operating at 400.33 MHz and equipped with a 5mm Bruker multinuclear z-gradient direct cryoprobe-head capable of producing gradients in the z direction with strength 53.5 G cm^{-1}. Each sample was dissolved in 0.4 mL of deuterated water for internal lock and spinning was used to minimize convection effects. The DOSY spectra were acquired with the *ledbpgp2s* pulse program from Bruker topspin software. The duration of the pulse gradients and the diffusion time were adjusted in order to obtain full attenuation of the signals at 95 % of maximum gradient strength. The values were 3.6 ms for the duration of the gradient pulses and 100 ms for the diffusion time. The gradients strength was linearly incremented in 16 steps from 5 % to 95 % of the maximum gradient strength. A delay of 3 s between echoes was used. The data were processed using 8192 points in the F2 dimension and 128 points in the F1 dimension with the Bruker topspin software. Field gradient calibration was accomplished at 25°C using the self-diffusion coefficient of H_2O+D_2O at 19.0 x 10^{-10} m^2.s^{-1}.

2.10. Thermogravimetric analysis

Thermogravimetric analyses were carried out using a Q50 TA instrument to assess the temperature stability of chitosans as well as determining the water content. Analyses were performed from 25 to 150°C with a temperature ramp of 2°C/min under a nitrogen flow.

2.11. Light scattering analysis

The water-solubility of chitosan and copolysaccharides at different pHs was assessed by light scattering (LS) measurements. Chitosan and copolysaccharide solutions prepared at 2 g/L in milli-Q water were adjusted at different pH values with 0.1 M NaOH. The light scattering intensity (kilo counts per second, kcps) was determined at 25°C using a ZetaSizer Nano ZS (Malvern Panalytical Ltd, Malvern, UK) working at λ = 632.8 nm with a back-scattering angle detection (173°). The average scattering intensity

is given by the derived count rate (DCR), taking into account the attenuation factor selected by the instrument.

2.12 Formation of copolysaccharide nanoparticles by nanoprecipitation

Copolysaccharides were dissolved at 1 g/L in milli-Q water and the solutions were adjusted at pH 4. 50 µL of the copolysaccharide solution were added to 450 µL of 50 mM MOPS buffer at pH 7.4 containing 100 mM NaCl. The addition was performed under fast mixing conditions. The solution was left under stirring for one hour and then analyzed by dynamic light scattering at 25°C using a ZetaSizer Nano ZS, as described above. Three measurements of 10 runs of 10 seconds were performed for each sample. The particle size evolution was monitored for 72 hours.

3. Results and discussion

3.1 Preparation and characterization of chitosan

Chitosans of various DPs were obtained by nitrous acid depolymerization of a weakly acetylated chitosan (DA 4%) according to the method of Allan and Peyron (Figure 1a) (Allan & Peyron, 1995a, 1995b). Nitrous acid initiates the cleavage of 2-amino-2-deoxy-D-glucosidic bonds by nitrosation of the amino groups, leading to the loss of nitrogen with a ring contraction of the D-glucosamine to the 2,5-anhydro-D-mannose unit, denoted as the M-unit hereafter (Gemma et al., 2008). After precipitation in alkaline conditions and purification, chitosans were recovered in good mass yields (> 70%) in their neutral form. The chitosan structure was verified by ^{1}H NMR (Figure 1b). DP_n was determined from the integral ratio of the H_2 protons of GlcN units and the H_{3M} protons of the terminal M-unit located at 3.20 ppm and 4.46 ppm, respectively. The DP values were adjusted by one unit to account for the presence of the terminal M-unit. SEC-MALS analysis evidenced that chitosans have relatively narrow molar mass distributions associated with dispersities (Đ) below 1.5 (Figure 1c). Overall, there is a good agreement between SEC-MALS and NMR on the DP values found in the range studied (Table 1). Chitosan blocks will be abbreviated as $Chit_m$ with m representing the DP value. The plot of DP as a function of the introduced GlcN/$NaNO_2$ molar ratio is linear, indicating that the depolymerization reaction is stoichiometric to the amount of $NaNO_2$ (Figure S2). TGA analysis of chitosans revealed that thermal degradation, which proceeds through cleavage of the glycosidic bonds (Wanjun et al., 2005) occurred more readily at lower temperatures when the DP is low (Figure S3). The degradation temperature, even for the chitosan with the lowest DP ($Chit_{19}$), was still above 150°C and therefore compatible for most applications.

The M-unit is of particular interest for hydrazone and oxime formation as the aldehyde groups is not involved in intramolecular hemiacetals as for a normal reducing end. Additionally, the M-unit does not undergo mutarotation in solution (Tømmeraas et al., 2001). Only the hydrated form of the aldehyde, the so-called *gem*-diol, could be detected on NMR spectra in D_2O at δ = 5.11 ppm (J = 5.5 Hz) (Figure 1b). Because of its high reactivity towards nucleophilic attacks, the M-unit is prone to form a Schiff base with the 2-amino groups of glucosamine units, giving rise to so self-branching structures, which may be of interest in the perspective of obtaining branched chitosans (Tømmeraas et al., 2002, 2011). The Schiff base can also initiate a degradation mechanism leading to chain cleavage with the formation of 5-hydroxymethylfurfural (HMF) (Tømmeraas et al., 2001). The formation of the Schiff base is favored under neutral/basic conditions while the degradation to HMF is catalyzed by acidic conditions. ^{1}H NMR analysis of $Chit_{25}$ at pH = 5.5 revealed the presence of minute amounts of imino protons (-C*H*=N-) at 8.1 ppm, (Tømmeraas et al., 2001) which probably result from the purification step when chitosan was precipitated under alkaline conditions (Figure S4). For pH below 4.0, the imine groups were no longer detected, but HMF formation could be observed (Figure S4) (Chapelle et al., 2019; Tømmeraas et al., 2001). However, the amount of HMF at pH = 1.0 was negligible (< 2 %), indicating that the M unit is readily available for subsequent coupling reactions. As the precipitation of chitosan in alkaline conditions was carried out rapidly, it is likely that this significantly prevented the formation of Schiff

bases and subsequent degradation into HMF under acidic conditions. It is important also to note that the stability of chitosan at the dried state depends on storage conditions. NMR analysis at pH 4.5 reveals a significant release of HMF (6 %) in chitosan stored for 6 months at room temperature or 4°C (Figure S5). However, no observable changes are noted for chitosan stored for 2 years at -20°C.

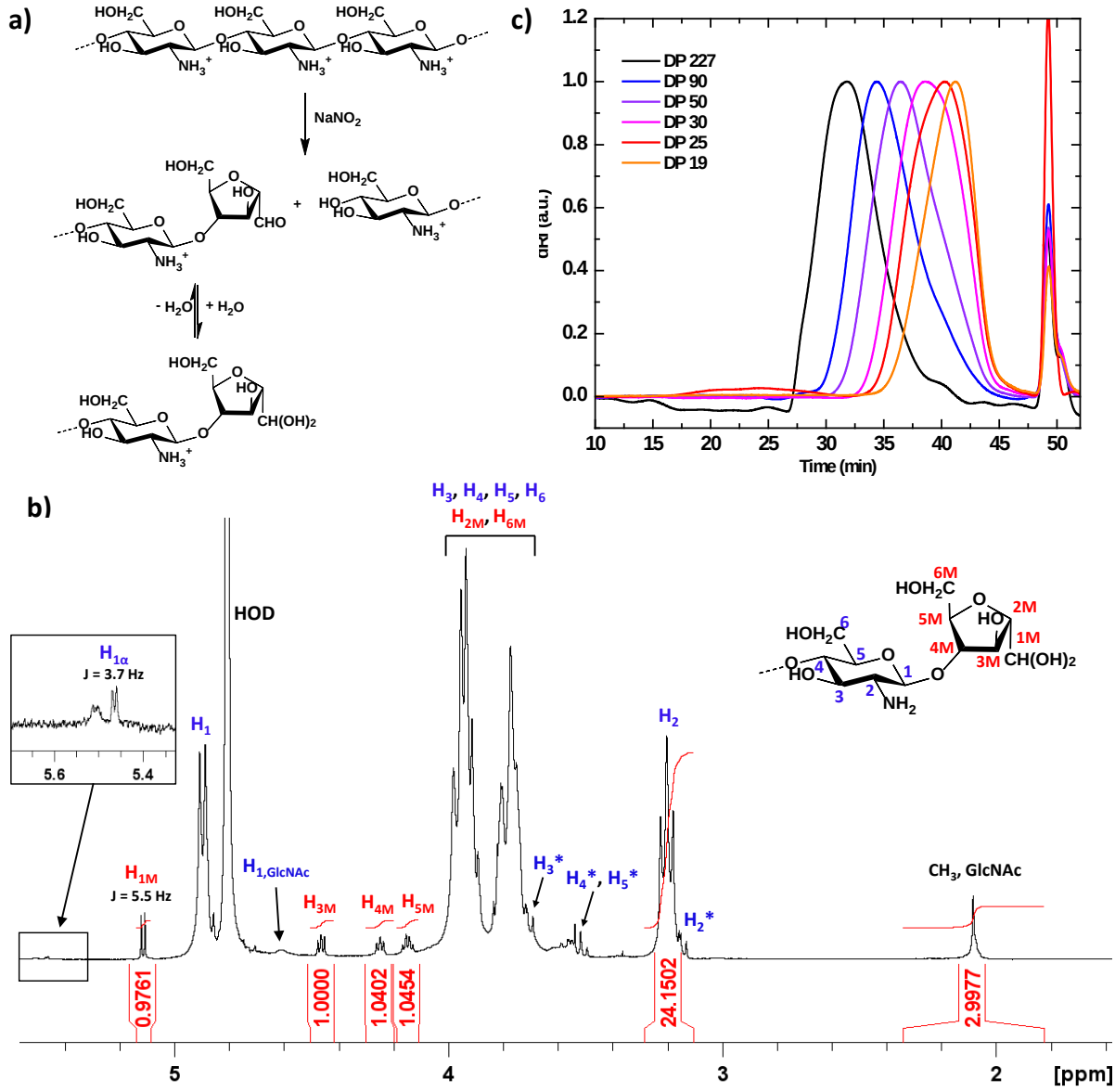

Figure 1. a) Chitosan depolymerization with sodium nitrite in acid conditions. The aldehyde group in the 2,5-anhydro-D-mannose (M) reducing end is predominantly in its hydrated form (gem-diol). b) ^{1}H NMR spectrum of $Chit_{25}$ in D_2O at pH 4.0 (H*: protons of the GlcN unit at the non-reducing end). See References (Coudurier et al., 2020; Tømmeraas et al., 2001) for peak assignments. c) SEC traces (dRI signal) of chitosans varying in DP in acetate buffer pH 4.5. Each chromatogram is scaled against its own magnitude.

Table 1. Characteristics of chitosans obtained by ^{1}H NMR, SEC-MALS and TGA analysis.

Name	M_n (g/mol) (SEC)	M_w (g/mol) (SEC)	Đ (SEC)	dn/dc[a] (mL/g)	DP_n (SEC)	DP_n (^{1}H NMR)	Water content (%)[b]
$Chit_{252}$	41,000	68,600	1.64	0.1876	252	-	7.9
$Chit_{90}$	15,000	23,100	1.54	0.1873	92	90	7.6
$Chit_{50}$	7,800	10,100	1.30	0.1858	48	50	10.2
$Chit_{30}$	5,100	6,500	1.27	0.1890	31	30	4.5
$Chit_{25}$	4,300	5,600	1.31	0.1912	23	25	5.0
$Chit_{19}$	3,200	3,700	1.17	-	20	19	9.8

[a] *analysis in acetate buffer pH 4.5*
[b] *determined by TGA at 150°C*

3.2 Characterization of dextrans

Four samples of dextran with molar masses of 5 kg/mol, 10 kg/mol, 20 kg/mol, and 40 kg/mol as indicated by the manufacturer, corresponding to theoretical DPs of 31, 62, 123 and 246 were selected for end-to-end coupling with chitosan. For linear block copolymers made from polystyrene and amine-terminated dextran, Bosker *et al.* reported that attempts to couple long dextrans (DP 58-123) failed (Bosker et al., 2003). Here, it is expected that the higher reactivity of the hydrazide and oxyamine groups compared to amines with the reducing end of dextran will allow the coupling of relatively long dextran blocks. Dextrans were characterized by ^{1}H-NMR in D_2O and SEC-MALS in phosphate buffer (Figure 2 and Table 2). The reducing end of dextran is a α/β-D-glucopyranose in equilibrium with the open aldehyde form, the latter represents only a very small fraction, < 0.002 % for glucose in aqueous solution (Dworkin & Miller, 2000). No aldehyde peak was found by NMR in dextran samples. The α/β anomeric protons of the reducing end could be well seen at δ = 5.26/4.69 ppm, even on the longest dextran (T40) (Figure 2). The peak at 5.34 ppm corresponds to the protons of α(1→3)-linked glycosyl units attached to the α(1→6) glycosyl units of the main chain. The degrees of branching (DB) were then determined from the integral ratio of α(1→3) protons and total anomers (Cheetham et al., 1990). The values of DB were observed to increase slightly from 1.8% to 3.5% as the molar mass of dextran increases (Table 2). While these values fall within the range typically obtained for dextrans, the correlation with molar mass has not been systematically observed (Benzeval et al., 2012). SEC-MALS analysis showed that all the dextran samples have relatively narrow molar mass distributions with dispersities (Đ) below 1.5 (Figure 2 and Table 2). The weight-average molar masses (M_w) correspond well to the molar masses provided by the manufacturer. The DP values obtained by NMR were lower than those obtained by SEC, likely due to the low integral peak intensities of the anomeric protons used for the determination of the DP. As NMR has been used for the determination of the yields of polysaccharide conjugation with ADH/PDHA and polysaccharide coupling, the DPs obtained by NMR have been preferentially utilized in this work, even if they are underestimated. Hereafter, dextran blocks will be abbreviated as $Dext_n$ with n representing the DP value.

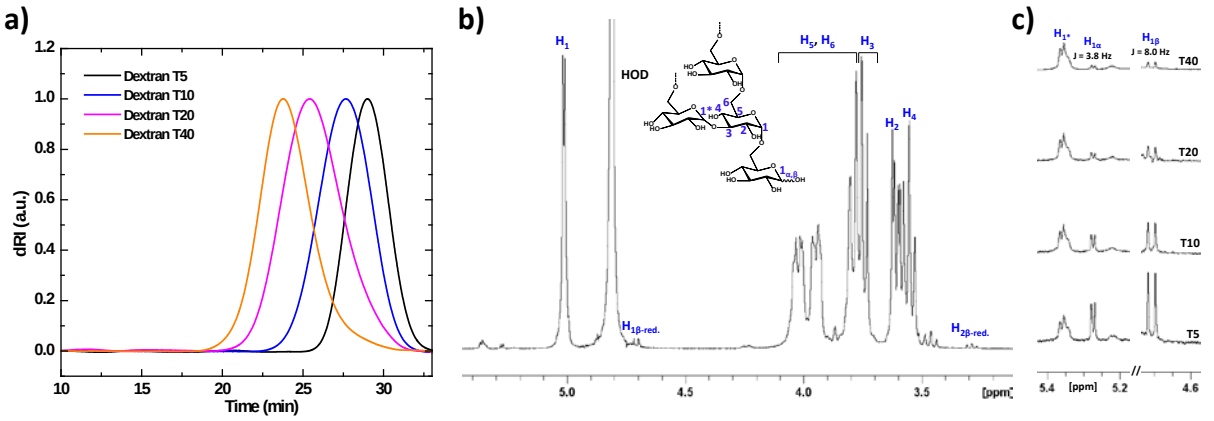

Figure 2. a) SEC traces (dRI signal) of commercial dextrans varying in molar mass in phosphate buffer pH 9. Each chromatogram is scaled against its own magnitude. b) ^{1}H NMR spectrum of dextran T10 in D_2O. See Cheetham et al., 1990 and Gagnaire & Vignon, 1977 for peak assignments. c) NMR signals of $H_{1,\alpha/\beta}$ protons at the reducing end of dextrans T5, T10, T20 and T40.

Table 2. Characterization of dextrans by ^{1}H NMR, and SEC-MALS.

Name	Commercial name	M_n (g/mol) (SEC)	M_w (g/mol) (SEC)	Đ (SEC)	dn/dc (mL/g)	DP_n (SEC)	DP_n (^{1}H NMR) [a]	DB (%) (^{1}H NMR) [b]
$Dext_{20}$	Dextran T5	4,400	5,200	1.19	0.1311	27	20	1.8
$Dext_{41}$	Dextran T10	8,100	10,600	1.30	0.1354	50	41	2.5
$Dext_{86}$	Dextran T20	16,600	23,900	1.44	0.1373	102	86	3.5
$Dext_{152}$	Dextran T40	37,800	42,200	1.11	0.1321	233	152	3.5

[a] *Degree of polymerization,* $DP = (I_{H1*} + I_{H1,\alpha/\beta} + I_{H1}) / I_{H1,\alpha/\beta}$
[b] *Degree of branching,* $DB = I_{H1*} / (I_{H1*} + I_{H1,\alpha/\beta} + I_{H1})$

3.3. End-functionalization of dextran and chitosan with ADH/PDHA

General considerations. The ultimate goal is to synthesize linear block copolysaccharides comprising a chitosan block and a dextran block, with one of their reducing ends requiring functionalization for subsequent coupling of the second block. Four potential copolymer synthesis routes were identified: ADH/PDHA end-functionalized dextran can react with chitosan, or ADH/PDHA end-functionalized chitosan can react with dextran (Scheme 2). The end-functionalization of chitosan and dextran blocks with ADH/PDHA is therefore a prerequisite before studying the coupling itself. Previous research works using short oligosaccharides blocks (DP ≤ 5) fractionated by gel filtration chromatography have allowed to investigate some important aspects of conjugation reactions with ADH/PDHA (Mo et al., 2020; Vikøren Mo et al., 2020): i) the various tautomeric forms of the *N*-glycosides studied, which exist as equilibrium between acyclic E/Z hydrazones (or oximes) and cyclic α/β-*N*-pyranosides or α/β-*N*-furanosides have been identified by NMR. ii) The formation of oxime and hydrazone typically exhibits a bell-shaped pH-rate curve, reaching a maximum at pH 4.0-5.0 (Jencks, 1964). This corresponds to the requirement of having the nucleophilic reagent in its basic form and maintaining acid-catalyzed conditions for the dehydration of the carbinolamine intermediate, which is the rate-determining step in imine formation (Jencks, 1964). A pH value of 4.0 was previously determined to be suitable for achieving high reaction yields and high reaction rates in both the functionalization of the reducing end with ADH/PDHA and its subsequent reduction (if required). Under such pH conditions, the amine groups of both ADH (pK_a = 3.1) and PDHA (pK_a = 4.2) are more nucleophilic than the amine groups of chitosan (pK_a ~ 6.5) (Vikøren Mo et al., 2020), thereby preventing self-branching reactions. From this perspective, hydrazide and oxyamine reagents are well-suited for modifying the reducing end of

chitosan. iii) Sodium cyanoborohydride ($NaBH_3CN$) is a suitable reducing agent to form stable secondary amine in high yields. The cyano ligand makes $NaBH_3CN$ a weak hydride source reacting with most easily reducible functional groups such as iminium ions, while reacting more slowly with ketones or aldehydes (Borch et al., 1971; Lane, 1975). Even though the choice of this reducing agent is questionable due to its toxicity, its high solubility in water (212 g/100 g water at 29°C) (Lane, 1975) ensures complete removal during purification steps. No trace of $NaBH_3CN$ has ever been detected by NMR in the reduced conjugates. Picoline borane has previously been used as a reducing agent, but its low solubility in water limits its use to achieve complete and rapid reduction of imines at room temperature (Mo et al., 2020; Vikøren Mo et al., 2020). iv) The equilibrium constant of condensation reactions in aqueous conditions being typically low ($K \sim 10\text{-}100\ M^{-1}$) (Gudmundsdottir et al., 2009), the overall concentration of the reactants must be high to obtain good yields (Kwase et al., 2013). The reaction rates are also anticipated to increase with higher concentration of reactants. For polymers, it is not advisable to use excessively high concentrations to prevent viscosity issues. In this context, polymer concentrations of 20 g/L for chitosan and 60 g/L for dextran were used. Since there are no specific viscosity issues associated with high concentrations of low molecular reagents, 20 equivalents of ADH/PDHA relative to the molar concentration of polysaccharide blocks were systematically used to achieve high conjugate yields. A high number of equivalents of ADH/PDHA also accounts for a low occurrence of dimerization reactions of polysaccharide blocks, estimated to be close to 1% for 20 equivalents, as theoretically calculated (Supporting Information S2). Regarding NMR data analysis, it is important to mention that the accuracy on peak determination and integral values cannot be as good as the one obtained with low DP oligosaccharides ($DP \leq 5$) (Baudendistel et al., 2016; Vikøren Mo et al., 2020). However, the characteristic peaks of the conjugates could be well identified, even with the longest dextran (T40), and the integrals were satisfactorily evaluated.

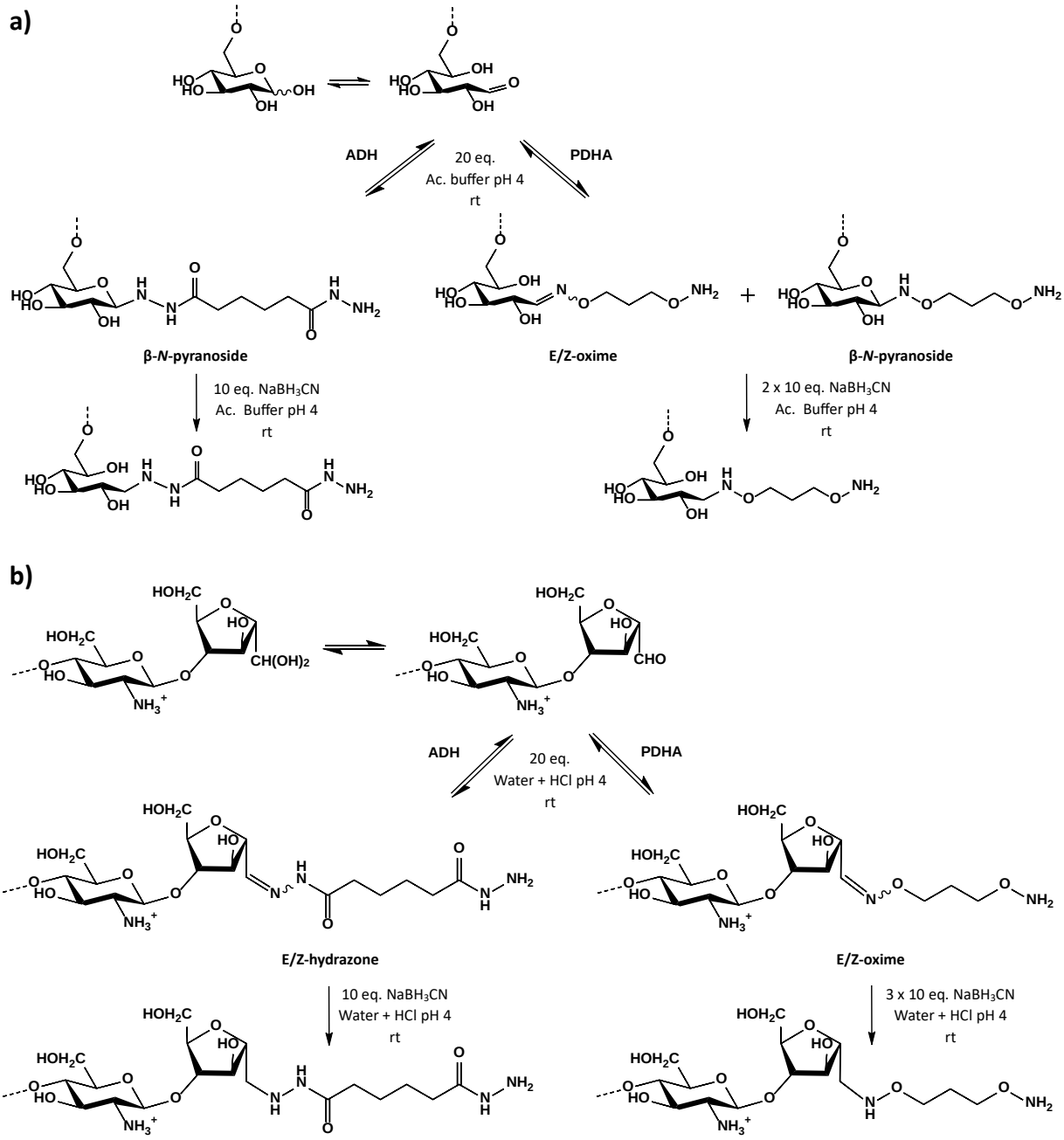

Scheme 2. End-functionalization of dextran (a) and chitosan (b) with ADH/PDHA under the conditions employed in this study. Only the main tautomeric forms of *N*-glycosides that were previously identified are depicted (see text).

Non reduced conjugates. Under the aforementioned conditions the modification of the reducing end of dextran and chitosan was first studied under non-reductive conditions. All experiments were performed with the $Dext_{41}$ and $Chit_{25}$ as reference samples. The structural characterization of conjugates was carried out by ^{1}H NMR. The kinetics of conjugation were monitored by performing time course NMR analysis directly in the mixtures of polysaccharide containing excess ADH/PDHA (Baudendistel et al., 2016; Mo et al., 2020; Vikøren Mo et al., 2020). Starting with the conjugation of dextran with ADH, only the cyclic β-*N*-pyranoside form could be evidenced on the purified conjugate (Figure 3a), as found for most of glycosyl hydrazides formed in aqueous solutions (Gemma et al., 2008; Kwase et al., 2013) and particularly with ADH (Cheng et al., 2019).

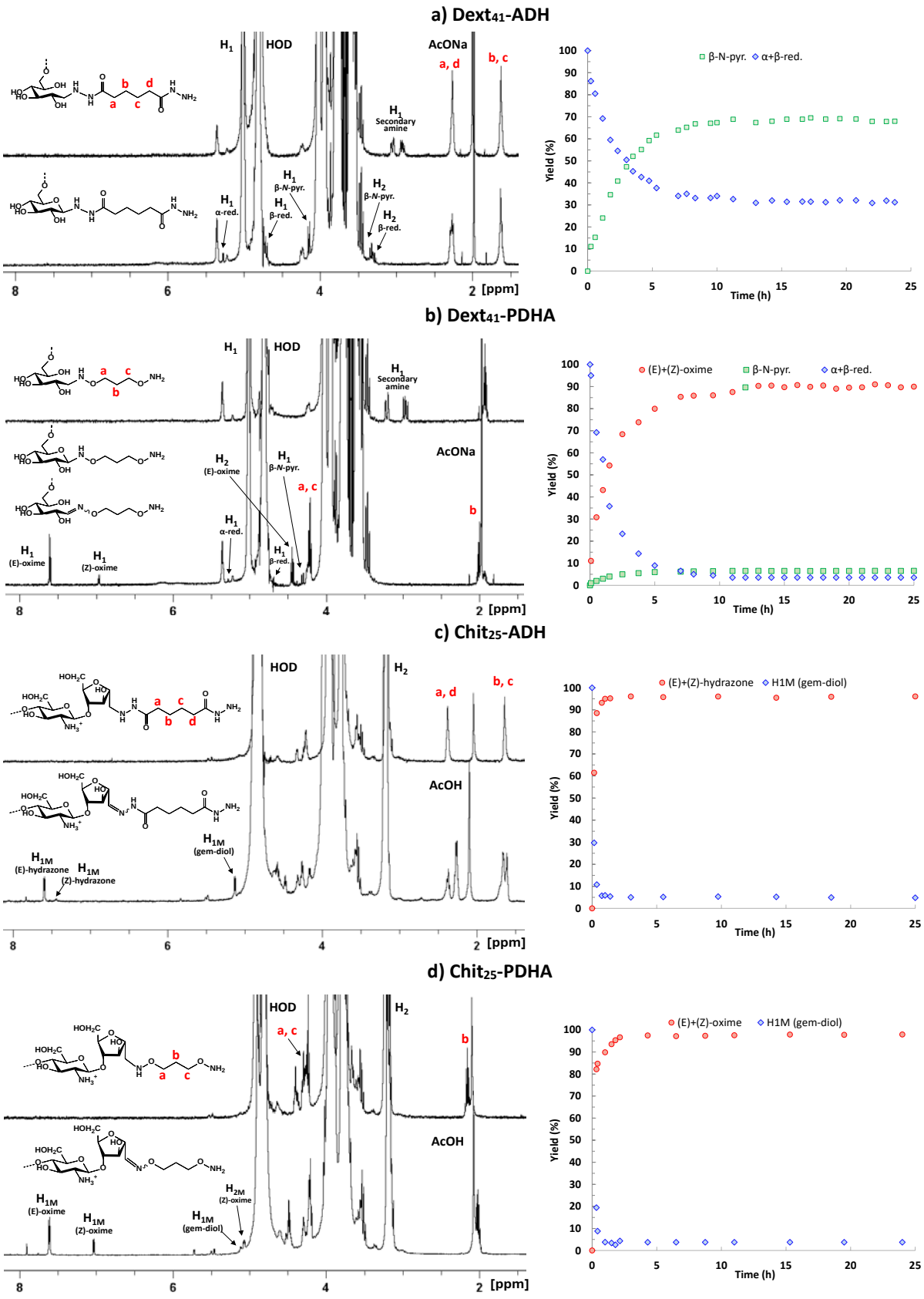

Figure 3. ^{1}H NMR analysis of purified $Dext_{41}$ and $Chit_{25}$ conjugates with ADH/PDHA. (Left) Non-reduced (bottom) and reduced (top) conjugates. (Right) Time course analysis of the reaction mixtures for the conjugation of $Dext_{41}$ and $Chit_{25}$ with ADH/PDHA under non-reductive conditions in D_2O at pH 4. The peak splitting of ADH signals observed in the non-reduced chitosan conjugates is pH dependent (see Figure S9).

It is assumed that the glycosyl hydrazide formation proceeds through the intermediate acyclic E/Z hydrazone before the ring closes to form the pyranose configuration. The coupling constant (J = 9.1 Hz) indicates a β-configuration, likely due to the conformational preference for equatorial positioning of substituents. The maximum yield, achieved after 10 hours of reaction of dextran with ADH, was approximately 70%, as determined from the integrals of either the β-*N*-pyranoside protons at 4.1 ppm or the sum of unreacted α/β anomeric protons in the mixture of dextran and excess ADH (Figure 3a and Figure S6a). This conjugation yield was also confirmed by more accurate integration of methylene peaks of ADH at 1.61 ppm and 2.25 ppm in the purified conjugate (Figure 3a). For PDHA, the signals of E/Z oxime and β-*N*-pyranoside could be detected in a ratio of (7:1) in the purified conjugate (Figure 3b), in close agreement with previous data obtained with the dextran of DP 5 (Mo et al., 2020). After 10 hours of reaction, the maximum yield of oxime formation reached nearly 90%. Considering both oxime and pyranoside peaks in the purified conjugate, the total conversion yield approaches 100%. In addition to achieving higher conjugation yields than ADH, PDHA also exhibits faster conjugation kinetics, as indicated by the $t_{0.9}$ values (Table 3). For chitosan, the distinctive configuration of the M-unit implies the exclusive formation of E/Z hydrazone and E/Z oxime with ADH and PDHA, respectively (Scheme 2). This was well verified by ^{1}H NMR of the purified conjugates (Figures 3c and d). The conjugation yields are close to 100%, as determined from the NMR data obtained in the equilibrium mixtures with an excess of ADH/PDHA (Figure S6c and S6d). However, upon purification of the conjugates we observed the gem-diol signal at 5.1 ppm for chitosan-ADH (Figure 3c). This suggests that the hydrazone linkage was not stable in the absence of excess ADH. Using an excess of ADH allowed to shift the equilibrium towards complete conjugate formation in the reaction mixture, ensuring the stability and high yield of the final product. Additionally, the pH of the chitosan solution must influence the hydrolytic stability of the hydrazone (See section 3.3.3). Here the, pH was adjusted to 5.5 for NMR analysis to minimize hydrolysis while ensuring chitosan solubilization.

Table 3. Reaction yields and kinetic parameters from time course NMR analysis of the conjugation reactions of $Chit_{25}$ and $Dext_{41}$ with 20 equivalents of ADH and PDHA.

Reaction	pH	$t_{0.5}$ (h)[a]	$t_{0.9}$ (h)[a]	Conjugate yield (%)
$Dext_{41}$-ADH	4.0	1.72	5.75	69
$Dext_{41}$-PDHA	4.0	0.95	3.17	97
$Chit_{25}$-ADH	4.0	0.10	0.34	96
$Chit_{25}$-PDHA	4.0	0.12	0.41	97

[a] $t_{0.5}$ and $t_{0.9}$: time to achieve 50% and 90%, respectively, of the maximal conversion.

Regarding the kinetic parameters of the conjugation, the values of $t_{0.5}$ and $t_{0.9}$ obtained for chitosan in the equilibrium mixtures with excess ADH/PDHA were significantly lower than those achieved with dextran, which is consistent with the greater availability of the aldehyde group at the reducing end of chitosan compared to dextran. The overall yields and kinetic constants obtained in this study with $Chit_{25}$ and $Dext_{41}$ are reasonably consistent with those previously obtained with oligosaccharide blocks of DP ≤ 5 (Mo et al., 2020; Vikøren Mo et al., 2020). This suggests that the conjugation reaction with ADH/PDHA is essentially independent of DP of polysaccharide block in the range studied.

For comparison purposes, the functionalization of the reducing end of dextran was carried out using 1,4-diaminobutane under similar conditions, with variations in the pH of the reaction medium (Figure S7). The reaction yield was notably low (~5%) at pH 4 and only slightly increased (~15%) at pH 8 due to the lower protonation rate of amine groups at this pH (pK_a diaminobutane = 10.8). This clearly demonstrates the inability of a primary amine with a pK_a around 10 to react effectively with the reducing end of dextran under non-reducing conditions. Dextran functionalization with diaminobutane was also

attempted in borate buffer at pH 8.5, which is known to increase the availability of the aldehyde at the reducing end (Levy & Doisy, 1928; Roy et al., 1984). However, the resulting dextran solution was too viscous under the conditions used for accurate NMR analysis (result not shown). For $Chit_{25}$, the end-functionalization with diaminobutane was tested at pH 5.5 to preserve good solubility properties of chitosan. However, the conjugation yield was found to be zero, as indicated by the unchanged integral of the gem-diol signal (Figure S7). Clearly, ADH, and even more so PDHA, with respective pK_a values of 3.1 and 4.2 (Vikøren Mo et al., 2020), emerge as much better candidates for the functionalization of the reducing end of polysaccharides under non-reducing conditions.

pH stability of the non-reduced conjugates. The limited stability of the hydrazone linkage at pH 5.5 obtained with chitosan-ADH prompted us to study the pH stability of non-reduced conjugates. Dextran and chitosan conjugates were dissolved in D_2O, and the pH of polymer solutions was adjusted with DCl to various values. The NMR spectra of conjugates were recorded 12 hours after pH adjustment (Figures S8 and S9). The intensity of proton signals associated with the E/Z oxime, E/Z hydrazone, and β-*N*-pyranoside groups decreased when the pH was reduced. Conversely, the intensity of the signals associated to the anomeric protons at the reducing end of dextran and the gem-diol proton of the M-unit increased as the pH decreased. Both variations evidence the cleavage of the β-*N*-pyranoside/hydrazone/oxime bonds in acidic conditions with the concomitant regeneration of the native reducing end. The relative abundance of the different forms of the reducing unit was estimated by NMR at different pHs (Figure 4).

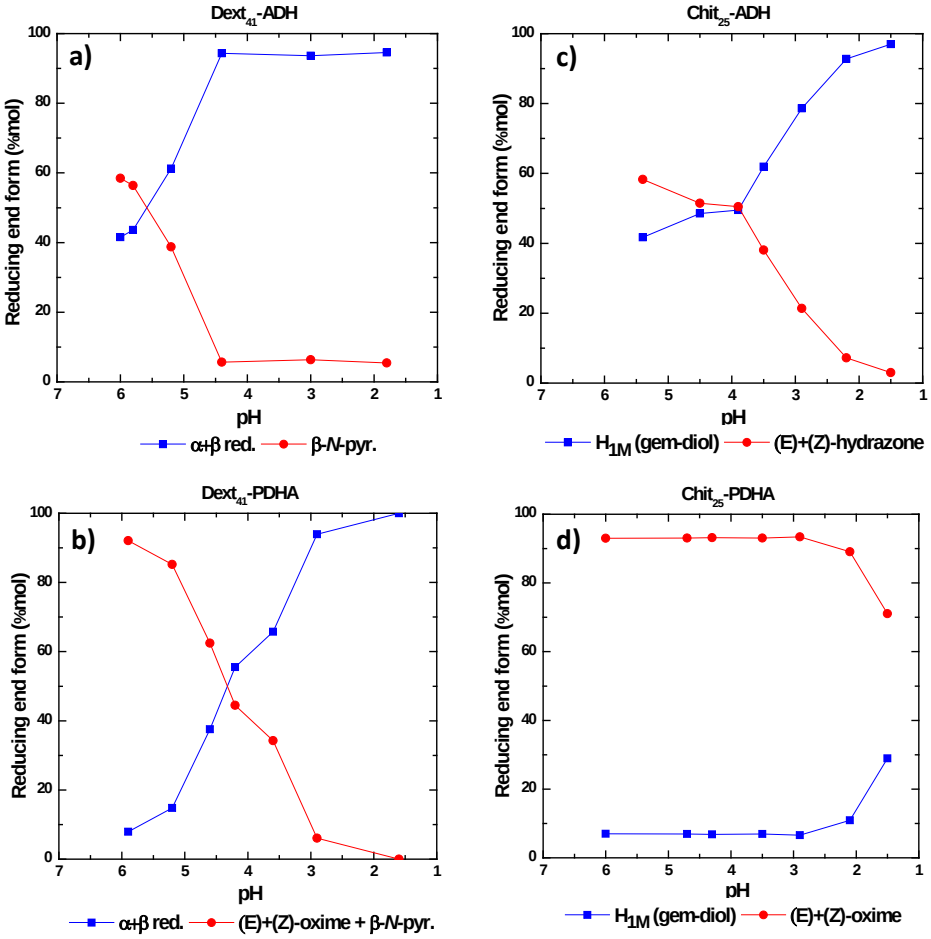

Figure 4. pH stability of the non-reduced conjugates. The abundance (in mol%) of the different forms of the reducing end, whether free or conjugated to ADH/PDHA, is represented as a function of the pH. a) $Dext_{41}$-ADH, b) $Dext_{41}$-PDHA, c) $Chit_{25}$-ADH and d) $Chit_{25}$-PDHA. Spectra were recorded 12 hours after pH adjustment.

Oxime bonds obtained from PDHA conjugates proved to be more stable than hydrazone bonds: the pH values required to achieve 90% hydrolysis ($pH_{0.9}$) were 4.5 for $Dext_{41}$-ADH and 3.0 for $Dext_{41}$-PDHA. The nature of the reducing end also affects the hydrolytic stability of hydrazone and oxime bonds. For $Chit_{25}$-ADH, $pH_{0.9}$ was 2.5, which is two units lower than obtained for $Dext_{41}$-ADH. This difference is attributed to the higher reactivity of the unmasked aldehyde groups in the M unit compared to the less available aldehyde group at the reducing end of dextran. The most stable conjugate was $Chit_{25}$-PDHA with 70% of the oxime groups remaining intact at pH 1.5. While the hydrolytic stability of oxime is well known (Munneke et al., 2015), the comparative stability of hydrazone and oximes has been less studied (Gudmundsdottir et al., 2009; Kalia & Raines, 2008). It has been suggested that oximes have greater hydrolytic stability than hydrazones due to their higher resistance to protonation (Kalia & Raines, 2008).

Reduced conjugates. The reduction of hydrazone or oxime functions was performed by adding a large excess of $NaBH_3CN$. This reduction was conducted directly in the reaction mixture after 12 hours of reaction, rather than on purified conjugates, to ensure that the equilibrium was well shifted towards conjugate formation when $NaBH_3CN$ was added. Some side reactions have to be considered when it comes to the reduction step. At first the reduction of the M-unit of chitosan is relatively fast, occurring within approximately 10 hours with only 3 equivalents of $NaBH_3CN$ at pH 4 (Mo et al., 2020). In contrast, for dextran, the reduction of the reducing end is negligible at pH 4, even in presence of 20 equivalents of $NaBH_3CN$ where the decrease in peak intensity of H-1(α) anomeric protons was only 4% (Figure S10). Another side reaction is the self-branching of chitosan in presence of $NaBH_3CN$ (Bezrodnykh et al., 2018; Tømmeraas et al., 2002, 2011), which was well evidenced on $Chit_{25}$ by SEC-MALS in various conditions of pH (Figure S11 and Table S3). Lastly, the addition of $NaBH_3CN$ in large excess contributes to a significant increase in the pH of the reaction medium (Table S4). This effect can be mitigated by employing buffered conditions, as was done here with dextran. However, in the case of chitosan, the use of acetate buffer is not recommended due to its tendency to promote self-branching reactions (Tømmeraas et al., 2001). Therefore, the reduction of chitosan was preferably conducted in water by adjusting the solution to pH 4.0. In this condition, the pH increased up to 5.2 with addition of $NaBH_3CN$, which remains within acceptable limits to maintain the solubility of chitosan (Table S4).

For dextran or chitosan conjugates obtained with ADH, only 10 equivalents of $NaBH_3CN$ were required to reduce the N-pyranoside or hydrazone functions (Figure S12). In contrast, the complete reduction of oximes derived from PDHA required larger amounts of $NaBH_3CN$ (2 x 10 equivalents for dextran-PDHA and 3 x 10 equivalents for chitosan-PDHA), confirming their greater stability compared to hydrazone (Figure S12). The nature of the reducing end, whether it is the M-unit or a normal reducing end, also affects the reduction of the oxime bond. This is evidenced by the larger amount of $NaBH_3CN$ required to reduce chitosan-PDHA in comparison to dextran-PDHA (Figure S12). After purification, the chemical structure of the reduced conjugates was confirmed by NMR (Figures 3a and 3b). In particular, the proton resonance of the newly formed secondary amine was well identified in the area 2.8-3.4 ppm in dextran conjugates (Ridley et al., 1997). For chitosan conjugates, this resonance which is pH-dependent, can be masked by the resonance of the H_2 protons due to the acidic conditions used for NMR analysis. However, the secondary amine could be detected on 2D HSQC NMR spectra (Figure S13). The degree of functionalization of dextran conjugates after reduction was found to be close to 100 % for both ADH and PDHA, within the uncertainty of the NMR analysis. Clearly, for dextran-ADH, the reduction step allowed to shift the equilibrium towards complete conversion of the conjugate. SEC-MALS analysis revealed the absence of any dimerization of the conjugates with either ADH or PDHA (Figure S14). However, it was evident that $Dext_{41}$-PDHA and $Chit_{25}$-PDHA conjugates strongly interact with the column in acetate buffer pH 4.5, likely due to electrostatic interaction of protonated amines of PDHA with residual carboxylate groups of the stationary phase.

3.4. Synthesis of chitosan-b-dextran copolysaccharides

The two approaches for synthesizing chitosan-*block*-dextran copolysaccharides involved either reacting end-functionalized dextran with chitosan (coupling route I) or end-functionalized chitosan with dextran

(coupling route II). ADH and PDHA were compared as potential linkers, resulting in four possible coupling routes (Scheme 1). The overall copolymer concentration and the number of equivalents of excess compound were maximized to achieve high yields and fast kinetics, while avoiding excessively high reaction medium viscosity. Since the purification method of copolymers relies on their precipitation in basic conditions, it is preferable to use excess dextran rather than excess chitosan in the coupling reaction. In fact, dextran can be easily removed by centrifugal washings while chitosan, if introduced in excess, will co-precipitate along the copolymer. Therefore, the typical coupling conditions involve a concentration of chitosan (or chitosan-ADH/PDHA) of 20 g/L and 3 equivalents of dextran-ADH/PDHA (or dextran). All reactions were conducted at room temperature in milliQ water, with the pH of all solutions adjusted at 4.0 with HCl (acetate buffer was avoided to minimize self-branching reactions). The reducing agent ($NaBH_3CN$), added in variable amounts depending on the linker, was introduced after 12 hours of reaction to allow for the formation of hydrazone/oxime linkage before reduction. Coupling tests were initially performed with $Chit_{25}$ and $Dext_{41}$ before applying the methodology with optimized conditions to other block lengths to synthesize a library of copolysaccharides.

Coupling method I. The coupling of chitosan with dextran-ADH/PDHA blocks (in their reduced form) was first investigated in the above-mentioned conditions. The formation of the hydrazone/oxime bonds with the concomitant disappearance of the gem-diol peak, was clearly evidenced by NMR after 4 hours of reaction (Figure S15). The coupling yield, derived from the integrals of hydrazone/oxime bonds was approximately 80% with $Dext_{41}$-ADH and 90% with $Dext_{41}$-PDHA, within NMR uncertainty. The complete reduction of the block copolysaccharides required 1 x 10 equivalents of $NaBH_3CN$ with ADH and 5 x 10 equivalents of $NaBH_3CN$ with PDHA, with additions made at 12-hour intervals. After reduction, the copolysaccharides were purified by precipitation in alkaline conditions to remove excess dextran-ADH/PDHA. Surprisingly, the copolymer was found in the pellet, not the supernatant, indicating its inability to form micellar aggregates at high pH, contrary to what would be expected for a double hydrophilic block copolymer. Once recovered, the copolymers were characterized by ^1H NMR and SEC-MALS (Figure 5). For $Chit_{25}$-*PDHA*-$Dext_{41}$, the chitosan content in the copolymer was slightly higher than the theoretical value (37 wt.%), indicating the presence of trace amounts of free chitosan. The molar mass of the copolymer obtained by SEC-MALS closely matched the theoretical value (Table 4). DOSY analysis further confirmed the coupling of the two polysaccharide blocks (Figure S16). Conversely, for $Chit_{25}$-*ADH*-$Dext_{41}$, the chitosan content was higher than expected (Table 4). The molar mass of $Chit_{25}$-*ADH*-$Dext_{41}$ was also notably higher than the theoretical one, which can be only attributed to self-branching of chitosan despite conditions to minimize it (Table 4). Self-branching involves the intra/intermolecular reaction of lateral amine groups with the free M-unit. This was likely to occur with $Chit_{25}$-*ADH*-$Dext_{41}$ due to a combination of two factors: the significant hydrolysis rate of the hydrazone at pH 4.0 and the relatively lower excess of dextran-ADH (3 equivalents) compared to the 20 equivalents of ADH previously used to form the chitosan-ADH conjugates. Under such conditions, stable branched chitosan structures could form upon addition of the reducing agent, similar to those observed when $NaBH_3CN$ was added to chitosan solutions at pH 4.0 (Figure S11 and Table S3).

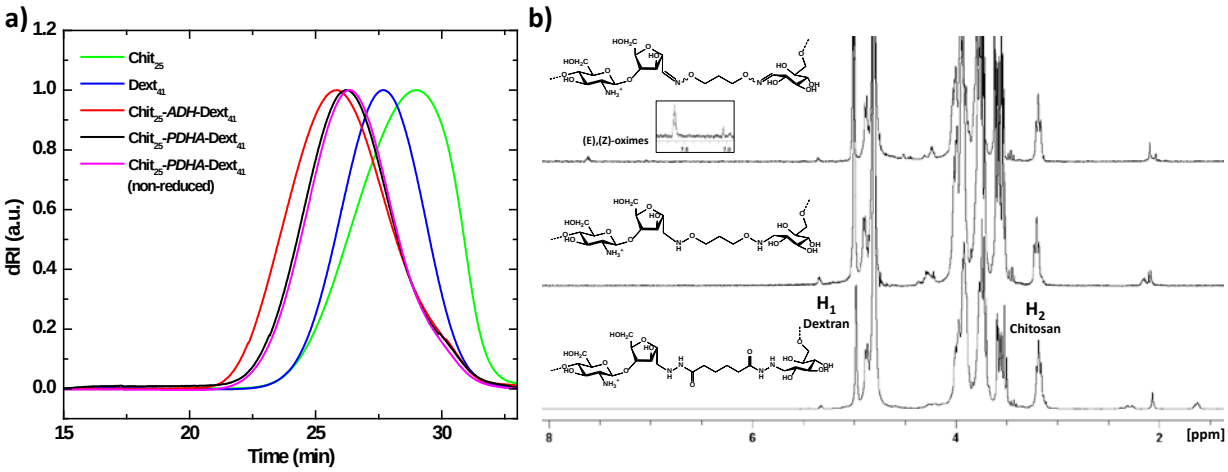

Figure 5. a) SEC traces (dRI signal) of polysaccharide blocks and block copolysaccharides in acetate buffer pH 4.5. Each chromatogram is scaled against its own magnitude. b) ^{1}H NMR spectra (from bottom to top) of reduced Chit$_{25}$-*ADH*-Dext$_{41}$, reduced Chit$_{25}$-*PDHA*-Dext$_{41}$ and non-reduced Chit$_{25}$-*PDHA*-Dext$_{41}$.

Table 4. SEC-MALS and ^{1}H NMR analysis of the block copolysaccharides (coupling method I) before purification.

Block copolysaccharide	Chitosan content [a] (wt.%)	$M_{n\ theoretical}$ (g/mol)	$M_{n\ SEC}$ (g/mol)	Đ
Chit$_{25}$-*ADH*-Dext$_{41}$	55	12,500	14,000	1.30
Chit$_{25}$-*PDHA*-Dext$_{41}$	43	12,500	11,700	1.20
Chit$_{25}$-*PDHA*-Dext$_{41}$ (non-reduced)	44	12,500	11,400	1.24

[a] obtained by NMR analysis, from the integral value of H_2 protons of chitosan and H_1 protons of dextran. The theoretical chitosan content is 38 wt.%, neglecting the contribution of ADH/PDHA.

Due to the relatively high stability of the intermediate oximes, the block copolysaccharide synthesis was attempted without any reduction step, which not only saved time but also eliminated the need for a toxic compound. The dynamic behavior of oxime bonds is also of interest to bring reversibility and self-healing properties (Mukherjee et al., 2014; Shen et al., 2018). The same reaction conditions were applied as previously described for the end-functionalization of the dextran with PDHA and its coupling with chitosan, except that both reduction steps were omitted from the protocol. After purification of the copolysaccharide by precipitation, NMR and SEC-MALS analysis evidenced that the coupling yield and molar mass of Chit$_{25}$-*PDHA*-Dext$_{41}$ were similar to those achieved in the presence of $NaBH_3CN$ (Figure 5 and Table 4). Therefore, the synthesis of block copolysaccharides under non reducing conditions is a viable approach when using PDHA as a linker.

For both the reduced and non-reduced Chit$_{25}$-*PDHA*-Dext$_{41}$ copolysaccharides, a small shoulder was visible on the low-mass side of the SEC chromatograms (Figure 5), indicating the presence of a small amount of unreacted chitosan. With the goal of achieving maximum purification of the copolysaccharides, two purification methods were tested with the reduced form of the copolymer. The first method utilized semi-preparative SEC, which proved to be effective on small amount of sample (Supplementary section S7). A more scalable method consisted in taking advantage of the enhanced water solubility of the copolymer compared to chitosan to extract free chitosan by selective precipitation. The pH of the Chit$_{25}$-*PDHA*-Dext$_{41}$ solution was set to 6.5 ± 0.1, slightly above the solubility pH of Chit$_{25}$ (Figure 9). After centrifugation, the polymer composition in the pellet and the supernatant was analyzed using SEC-MALS and NMR (Figure 6 and Table 5). The polymer in the supernatant had a

composition and a molar mass close to the expected copolymer structure. The polymer in the pellet consisted of free chitosan and copolysaccharide, accounting for 11 % of the total mass of non-purified copolymer. However, this amount increased up to 29 % at pH 7.0, indicating precipitation of a substantial copolymer fraction at higher pHs due to the insolubility of chitosan blocks (Table S6). Therefore, a pH of 6.5 seems appropriate to selectively remove excess chitosan by precipitation while only losing a small amount of copolymer. This pH is compatible with both $Chit_{25}$ and $Chit_{50}$ as their critical solubility pH are close to 6.5 (Figure 9). For chitosan blocks of shorter sizes (DP < 25), higher pH values would be required to selectively extract free chitosan, as their solubility increases significantly (Delas et al., 2019).

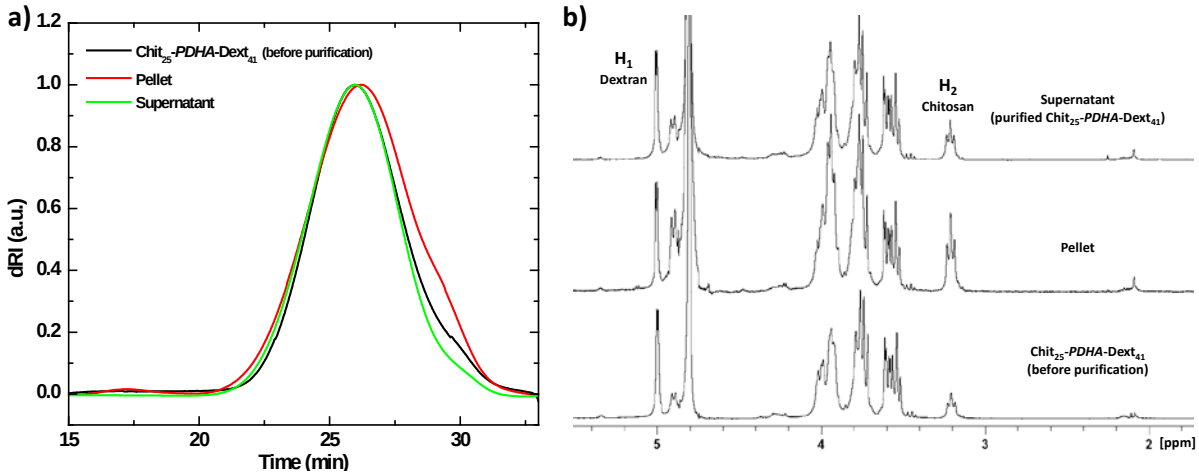

Figure 6. Analysis of $Chit_{25}$-*PDHA*-$Dext_{41}$ before and after precipitation/centrifugation at pH 6.5. a) SEC traces (dRI signal) in acetate buffer pH 4.5. Each chromatogram is scaled against its own magnitude. b) ^1H NMR spectra in D_2O.

Table 5. SEC-MALS and ^1H NMR characterization of the pellet and supernatant after precipitation/centrifugation of $Chit_{25}$-*PDHA*-$Dext_{41}$ at pH 6.5.

Sample	Chitosan content (wt.%)	$M_{n\ SEC}$ (g/mol)	Đ
$Chit_{25}$-*PDHA*-$Dext_{41}$ (before purification)	43	11,700	1.20
Pellet	58	9,900	1.27
Supernatant	40	12,000	1.23

Coupling method II. In a second approach, ADH/PDHA end-functionalized chitosan was reacted with dextran under similar experimental conditions of pH, temperature, and polymer concentrations (Figure 7a,b). Specifically, 1 equivalent of $Chit_{25}$-ADH/PDHA was reacted with 3 equivalents of $Dext_{41}$ at pH 4.0 with daily additions of 10 equivalents of $NaBH_3CN$. The kinetics of block coupling was slower compared to the previous approach due to the reduced availability of the aldehyde groups at the reducing end of dextran in comparison to the M unit of chitosan.

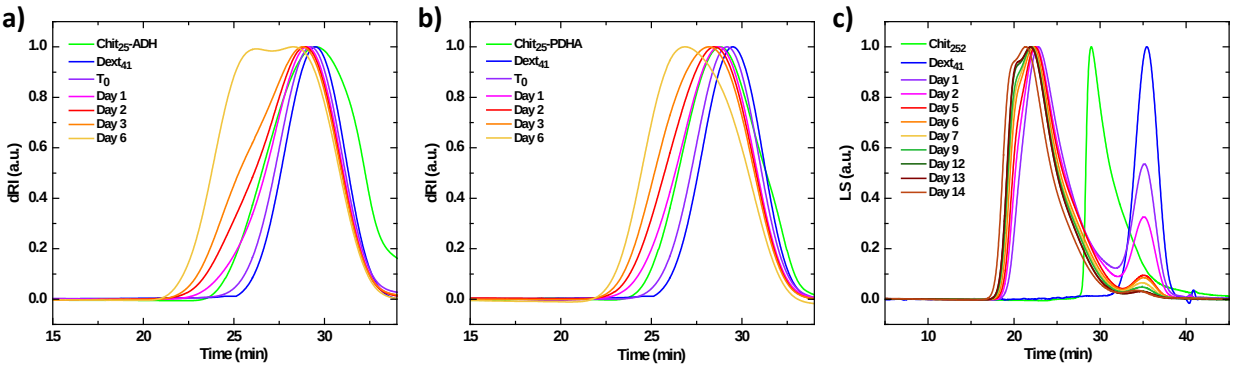

Figure 7. SEC monitoring (dRI signal) of the reaction of a) $Chit_{25}$-ADH + 3 eq. $Dext_{41}$, b) $Chit_{25}$-PDHA + 3 eq. $Dext_{41}$ and c) $Chit_{252}$ + 3 eq. $Dext_{41}$. All reactions were conducted under reductive conditions with daily additions of 10 eq. $NaBH_3CN$. For the reaction with $Chit_{252}$, the LS signal was more suitable than dRI to monitor the increase in molecular weight of dextran-*grafted*-chitosan copolymer. SEC analyses were performed in acetate buffer pH 4.5 by direct injection of the reaction mixture after appropriate dilution with the buffer. Each chromatogram is scaled to its own magnitude.

Table 6. SEC-MALS characterization of the grafted copolysaccharides (coupling method II).

Copolysaccharide	**$M_{n\ theoretical}$ (g/mol)**	**$M_{n\ SEC}$ (g/mol)**	**Đ**	**Branching degree (%)**
$Chit_{25}$-*ADH*-$Dext_{41}$ (day 6)	12,500	15,200	1.76	-
$Chit_{25}$-*PDHA*-$Dext_{41}$ (day 6)	12,500	14,600	1.60	-
$Chit_{252}$	-	41,000	1.40	-
$Dext_{41}$	-	8,100	1.22	-
$Dext_{41}$-*g*-$Chit_{252}$ (day 1)	-	221,000	2.54	8.8
$Dext_{41}$-*g*-$Chit_{252}$ (day 2)	-	292,000	2.05	12.3
$Dext_{41}$-*g*-$Chit_{252}$ (day 5)	-	402,000	2.74	17.7
$Dext_{41}$-*g*-$Chit_{252}$ (day 6)	-	410,000	2.23	18.1
$Dext_{41}$-*g*-$Chit_{252}$ (day 7)	-	445,000	2.69	19.8
$Dext_{41}$-*g*-$Chit_{252}$ (day 9)	-	631,000	2.55	28.9
$Dext_{41}$-*g*-$Chit_{252}$ (day 12)	-	610,000	2.35	27.9
$Dext_{41}$-*g*-$Chit_{252}$ (day 13)	-	793,000	2.63	36.8
$Dext_{41}$-*g*-$Chit_{252}$ (day 14)	871,000	810,000	2.27	37.6

Surprisingly, the molar mass of the copolymer obtained after 6 days exceeded the theoretical one expected for a linear $Chit_{25}$-*b*-$Dext_{41}$, using either ADH or PDHA as linker (Figure 7a,b and Table 6). Self-branching reactions cannot be considered due to the modification of the aldehyde group of the M-unit with ADH/PDHA. Therefore, the increase in molar mass can only be attributed to the grafting of dextran blocks onto the lateral amine groups of chitosan, in addition to chain-end coupling. This indicates that the hydrazide or oxyamine group at the chitosan chain-end could not outcompete the lateral amine groups in the modification of the reducing end of dextran, when performed under reducing conditions. This last point is particularly significant because, as shown previously, the amination of dextran or chitosan with diaminobutane results in zero or low yields under non-reducing conditions. From the literature, several studies have reported the covalent linking of reducing sugars, including dextran, to chitosan through reductive amination, specifically by using sodium cyanoborohydride (Janciauskaite et al., 2008; Yalpani & Hall, 1984). An attempt was made to graft dextran onto the starting

chitosan of 41 kg/mol ($Chit_{252}$), which lacks the M-unit at the reducing end. The number of equivalents of dextran chains relative to amine functions of chitosan was set to 1:2.5, with the experimental conditions being similar to those used before. As observed in Figure 7c, the amount of free dextran decreased over time while the molar mass of the copolymer increased (Table 6). After 14 days of reaction, nearly all the dextran chains were grafted onto the chitosan. The final degree of branching was then 38 %. In conclusion the second coupling route is not appropriate to synthesize linear block copolysaccharides from chitosan-PDHA and dextran. Using higher excess of chitosan-PDHA cannot be envisaged as the equivalent number of primary amine groups of chitosan will increase as well.

Library of chitosan-*b*-dextran and dextran-*g*-chitosan copolysaccharides. The optimal method for synthesizing linear block copolysaccharides involves reacting chitosan-M with three equivalents of dextran-PDHA in aqueous conditions at pH 4.0 and room temperature. The reduction, if needed, was achieved with 5 x 10 equivalents of $NaBH_3CN$. Different copolymer compositions were targeted from $Chit_{25}$ and $Chit_{50}$, along with $Dext_{20}$, $Dext_{41}$ and $Dext_{86}$, functionalized with PDHA. The copolymers under their reduced form were analyzed by SEC-MALS and ^1H NMR after extraction of unreacted chitosan at pH 6.5. The shift associated with the increase in molar mass could be clearly identified by SEC for all block copolymer compositions (Figure 8). The method used for the extraction of free chitosan by selective precipitation was found to be efficient for all copolymer compositions, as shown by a systematic decrease of the chitosan content after purification (Figure S20 and Table 7). However, it is worth noting that the final chitosan content can be influenced by copolymer fractionation at pH 6.5. Copolymer fractions containing larger chitosan blocks or higher chitosan contents tend to precipitate more effectively, resulting in a lower chitosan content in the purified copolymer (Table 7). From this view perspective, preparative gel filtration chromatography would be more suitable for purifying copolymers. Dextran-*grafted*-chitosan copolymers were also prepared with $Chit_{252}$ and $Dext_{41}$ with targeted branching degrees of 15, 25 and 40 %. After 14 days of reaction with daily addition of $NaBH_3CN$, the molar mass of copolymer agreed with a nearly quantitative reaction yield (Table 7).

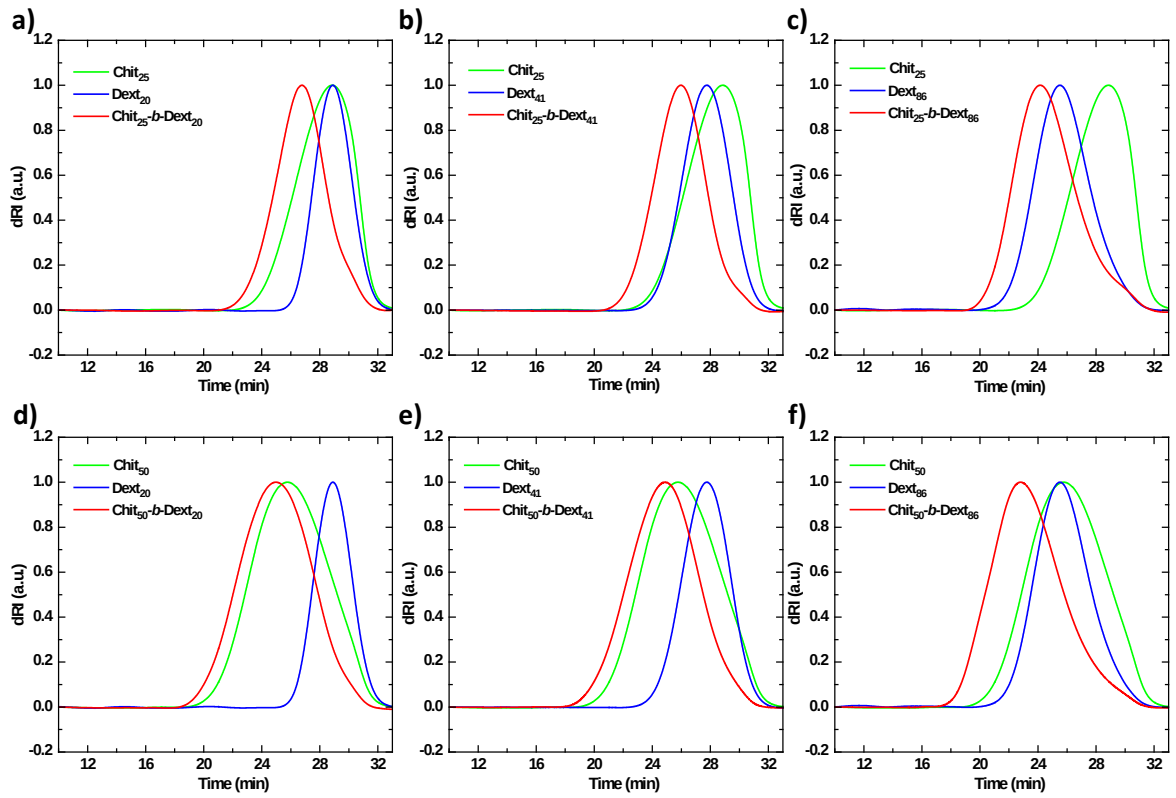

Figure 8. SEC traces (dRI signal) of purified block copolysaccharides and their precursors in acetate buffer pH 4.5. a) $Chit_{25}$-*b*-$Dext_{20}$, b) $Chit_{25}$-*b*-$Dext_{41}$, c) $Chit_{25}$-*b*-$Dext_{86}$, d) $Chit_{50}$-*b*-$Dext_{20}$ (not purified), e) $Chit_{50}$-*b*-$Dext_{41}$ and f) $Chit_{50}$-*b*-$Dext_{86}$.

Table 7. SEC-MALS and NMR characterization of the library of $Chit_m$-*block*-$Dext_n$ and dextran-*grafted*-chitosan copolysaccharides.

Copolysaccharide	M_n chitosan (g/mol)	M_n dextran (g/mol)	M_n copolymer (g/mol)	$Đ_{copolymer}$	$dn/dc_{copolymer}$ (mL/g)	Chitosan content (wt.%) Theory	Chitosan content (wt.%) Exp. [a]	Branching degree (%)
$Chit_{25}$-*b*-$Dext_{20}$	4,300	4,400	9,200	1.23	0.1479	55	49 (54)	-
$Chit_{25}$-*b*-$Dext_{41}$	4,300	8,100	12,000	1.23	0.1438	38	40 (43)	-
$Chit_{25}$-*b*-$Dext_{86}$	4,300	16,600	23,800	1.48	0.1366	22	28 (31)	-
$Chit_{50}$-*b*-$Dext_{20}$	7,800	4,400	14,700	1.44	0.1553	71	(70)	-
$Chit_{50}$-*b*-$Dext_{41}$	7,800	8,100	20,900	1.39	0.1459	55	53 (56)	-
$Chit_{50}$-*b*-$Dext_{86}$	7,800	16,600	37,900	1.51	0.1377	37	35 (35)	-
$Chit_{90}$-*b*-$Dext_{152}$	15,000	37,800	58,700	1.28	0.1363	37	21 (31)	-
$Dext_{41}$-g^{36}-$Chit_{252}$	41,000	8,100	770,000	2.30	0.1315			35.7
$Dext_{41}$-g^{22}-$Chit_{252}$	41,000	8,100	496,000	2.60	0.1296			22.3
$Dext_{41}$-g^{12}-$Chit_{252}$	41,000	8,100	293,000	2.58	0.1348			12.3

[a] after purification (before purification)

Finally, in order to test the robustness of the method I to synthesize linear block copolysaccharides with PDHA, the coupling was assessed with relatively high molecular weight polysaccharide blocks, namely a chitosan block of 14,000 g/mol ($Chit_{90}$) and a dextran block of 40,000 g/mol ($Dext_{152}$). For this experiment, the dextran was end-functionalized with PDHA under reducing conditions. The same block coupling conditions as described above (polymer mass concentration, number of equivalents, pH, reaction time) were applied, except that the temperature was set to 50°C for the oxime formation, due to increased viscosity of the reaction mixture. The progress of the reaction was monitored by NMR, as (E), (Z) oxime protons could be still detected (Figure 9). After reduction, the copolymer was recovered by precipitation and subsequently purified (Table 7). SEC-MALS and NMR indicated that the coupling was successful. However, the final chitosan content obtained in the copolymer after purification was low, likely due the poor solubility of the large chitosan blocks at pH 6.5.

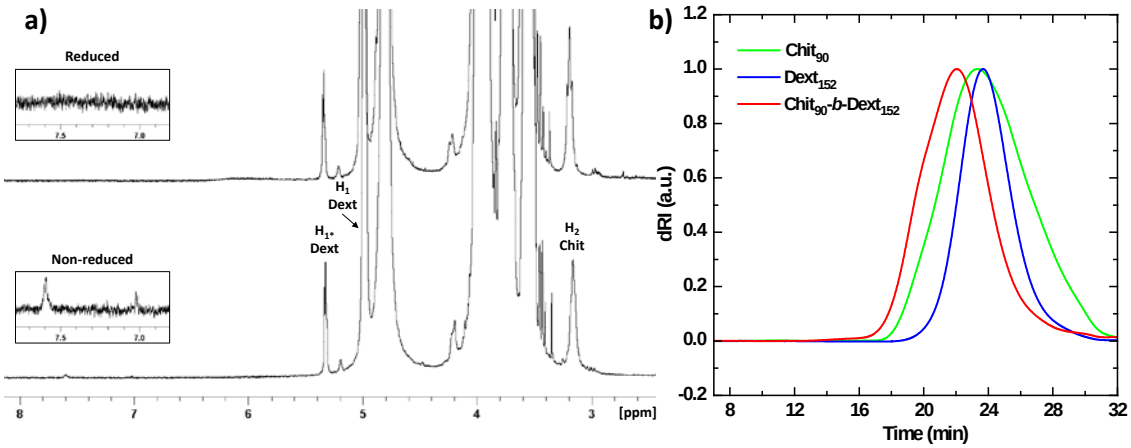

Figure 9. Synthesis and characterization of $Chit_{90}$-*b*-$Dext_{152}$. a) ^1H NMR of the reaction mixture containing $Chit_{90}$ + 3 eq. of $Dext_{152}$-PDHA, after 12 hour-reaction at 50°C (bottom) and after reduction with 5 x 10 eq. of $NaBH_3CN$ at room temperature (top). b) SEC traces (dRI signal) of purified $Chit_{90}$-*b*-$Dext_{152}$ and its precursors in acetate buffer pH 4.5.

3.5. Water solubility of chitosan-b-dextran copolysaccharides

The solubility of chitosan in water is influenced by both pH, molar mass and degree of acetylation (DA) (Delas et al., 2019; Qin et al., 2006; Vårum et al., 1994). For fully deacetylated chitosans we previously showed that the critical pH of solubility decreased from 7.5 to 6.0 when the DP increased from 5 to 50 (Delas et al., 2019). Since chitosan chains were linked with dextran, which is fully water soluble, it is expected that the solubility of the copolymers would increase accordingly. Specifically, we can anticipate these copolymers to be soluble under physiological conditions at pH 7.4, which would make them suitable for drug and gene delivery applications. The pH-dependence of the solubility was evaluated by light scattering, which is particularly sensitive to detect the collapse and aggregation of polymer chains at the molecular level through an increase of the scattering intensity. The most striking result is that the conjugation of chitosan to dextran blocks did not fully prevent the block copolysaccharides from undergoing macroscopic precipitation under neutral or basic conditions, even for the copolymers containing the highest mass fraction of dextran, *i.e.*, $Chit_{25}$-*b*-$Dext_{86}$ (Figure 10). From this viewpoint, chitosan-*b*-dextran did not exhibit the typical behavior of double hydrophilic block copolymers (DHBCs) based on a weak polybase like polyhistidine, poly(2-vinylpyridine) or poly(2-(diethylamino)ethyl methacrylate) linked to a hydrophilic block like PEO, which showed self-assembly properties into micellar or vesicular aggregates at pH above 8 (Borchert et al., 2006; Butun et al., 1998; Lee et al., 2003). This can be understood by considering that chitosan in their neutralized state can form cooperative intra- and intermolecular hydrogen bonds that are strong enough to significantly reduce the dynamics of the block copolymer chains, thereby preventing their self-assembly, which would have allowed for the observation of micellar structures at basic pHs. Increasing the degree of acetylation of chitosan could potentially compensate for this effect but has not been tested in the current study.

However, the coupling of chitosan with dextran accounts for an increase of their solubility range by at least one pH unit with the copolymer compositions tested here (Figure 10). The length of the dextran block has little influence on the critical pH of solubility of the copolymers, suggesting that the hydrogen bonds formed by chitosan govern the solution behavior of the copolymers. Therefore, it is rather the length of the chitosan block that exerts some influence on the solubility of the copolymers. While the critical pH values of $Chit_{25}$ and $Chit_{50}$ are nearly equal, the copolymers based on $Chit_{50}$ have critical pH values lower by 0.4 pH units compared to those formed from $Chit_{25}$ (Figure 10) The $Chit_{50}$-*b*-$Dext_{20}$ copolymer, which was not purified, has a critical pH of 6.3 due to the presence of free $Chit_{50}$ contributing to the early increase in scattering intensity (Figure 10). Thus, it is interesting to mention that light scattering is sensitive enough to detect the presence of free chitosan, and consequently this technique is suitable to assess the effectiveness of the copolymer purification procedure.

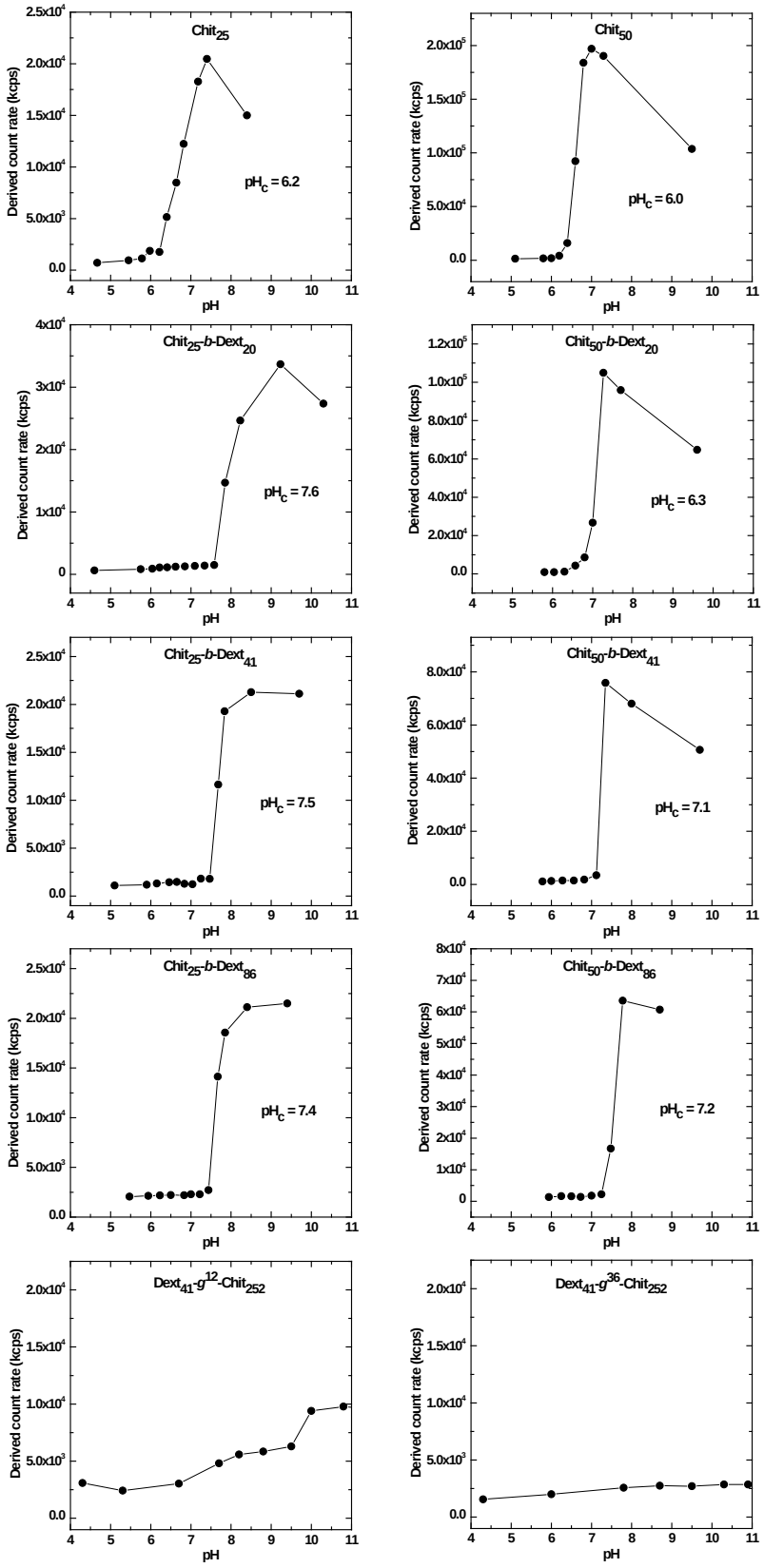

Figure 10. Variation of the scattered light intensity (in kcps, kilo count-per-second) of $Chit_m$-*b*-$Dext_n$ and $Dext_n$-g^x-$Chit_m$ copolysaccharide solutions at 2 g/L as a function of the pH. The critical pH (pH_c), corresponding to the onset of precipitation, is indicated on the graph.

As the light scattering measurements were performed with a DLS instrument, attention was also given to the correlograms, and particle size distributions obtained for the various copolymer compositions above the critical pH. Nanoparticles with diameters ranging from 350 nm to 400 nm could be obtained around pH 7.5, but only for copolymers containing the longest dextran blocks ($Dext_{86}$) (Figure 11). A nanoprecipitation approach was then carried out to assess the possibility of forming smaller nanoparticles by rapidly precipitating these copolymers at pH 7.4. In this process, the fast desolvation of the chitosan blocks by neutralization of the charged amino groups should promote the formation of particles with a high nucleation rate and should be therefore suitable for obtaining small particles. In practice this consisted in dissolving the copolymers at pH 4.0 and then rapidly mixing the copolymer solutions with an excess of 50 mM MOPS buffer at pH 7.4 containing 100 mM NaCl. This approach proved to be efficient to obtain relatively stable nanoparticles in the size range of 100 nm – 400 nm but only for copolymers based on the longest dextran block ($Dext_{86}$) (Figure 11). This can be understood by considering that once the particles nucleate, they have a strong tendency to aggregate through hydrogen bonding between the neutralized chitosan blocks. In such circumstances, the dextran blocks must be sufficiently long to create a steric barrier at particle surface able to generate strong repulsive forces to oppose particle aggregation (Johnson & Prud'homme, 2003). The particles obtained through nanoprecipitation are in a frozen state, meaning the dynamics of the copolymer chains is too low to establish an equilibrium state between the free unimers and the particles. To achieve true micellar aggregates in dynamic equilibrium, the dextran block length needs to be significantly longer, or the chitosan block length much shorter. Under such conditions, star-like micelles could be obtained.

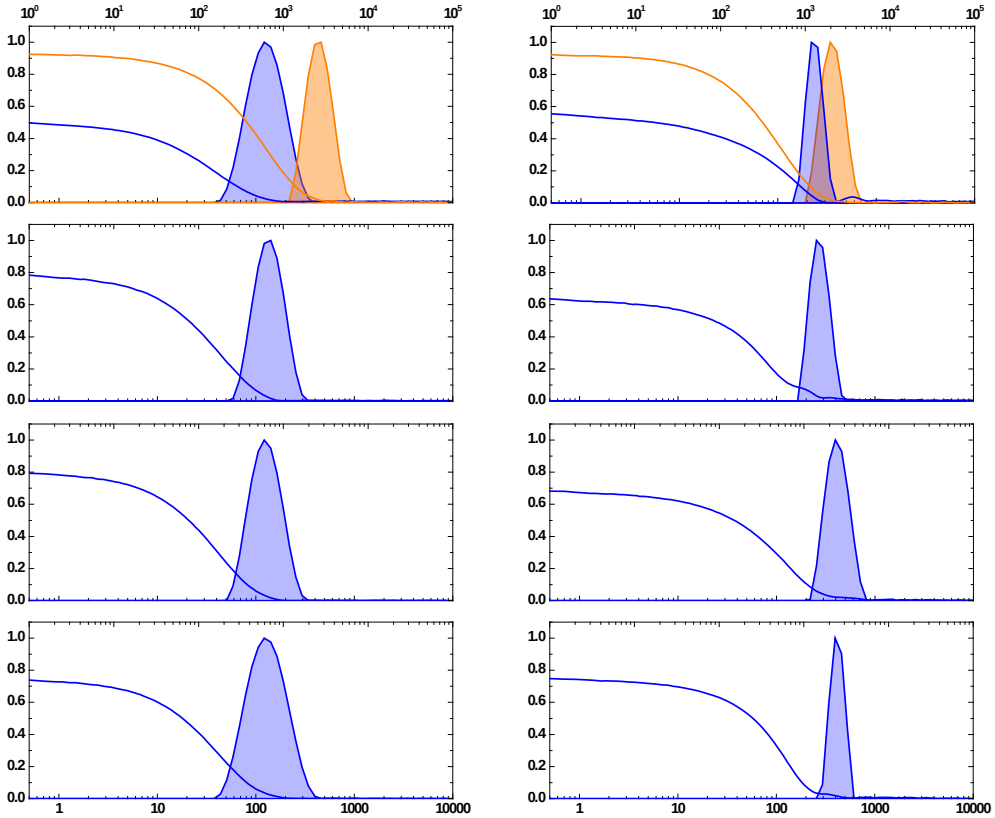

Figure 11. Dynamic light scattering analysis of the particles formed by increasing the pH of copolysaccharide solutions from 4.0 to 7.4: gradual pH increase (orange curves), nanoprecipitation approach (blues curves) by adding the copolysaccharide solution rapidly to 50 mM MOPS buffer at pH 7.4. Autocorrelation functions and size distributions are shown for two block copolysaccharide compositions. Stability of the particles obtained by nanoprecipitation was monitored over a period of 72 h.

The dextran-*grafted*-chitosan copolysaccharides exhibited a markedly different behavior within the composition range studied. The $Dext_{41}$-g^{36}-$Chit_{252}$ (DB = 36 %) remained well solubilized even at highly basic pH (Figure 10). A slight increase in scattering intensity could be observed for $Dext_{41}$-g^{12}-$Chit_{252}$ (DB = 12 %) but no precipitation occurred (Figure 10). The grafting of dextran branches not only enhance the hydrophilicity of chitosan, but also reduce the possibility of hydrogen bonding. This is due not only to the significant reduction in the number of free amino groups but above all to the presence of a steric brush layer around the chitosan chains, which prevents their aggregation under neutral and basic pH conditions. The enhanced water solubility of graft copolymers may be of interest for several applications as solution modifiers, especially in physiological conditions. However, the limited accessibility of amine groups will alter the complexing properties of chitosan.

4. Conclusion

In this work, we have described an approach for synthesizing linear block copolysaccharides from chitosan and dextran. The approach relies on the coupling of the reducing end of these polysaccharides with diamine linkers. This strategy presents several challenges. Firstly, the reducing ends of polysaccharides are not very reactive in aqueous media due to the low availability of the aldehyde form, which is in equilibrium with the hemiacetal form. For chitosan, however, a highly reactive M unit can be generated at the reducing end by degrading chitosan with nitrous acid. Conversely, dextran has a conventional, thus less reactive, reducing end. A second difficulty lies in the solubility properties of chitosan, which is only soluble in slightly acidic media, typically at pH below 6. This pH is unsuitable for the amination of the reducing ends with conventional diamines because they are protonated at this pH, making them less reactive, as confirmed with diaminobutane. Finally, when coupling large polysaccharide blocks, the probability of chain ends encountering is low and must be counterbalanced by a high reactivity of the linker. In this context, we have shown that dihydrazide (ADH) or dioxyamine (PDHA) diamines are much more suitable for polysaccharide coupling due to their high nucleophilicity and low basicity, allowing the coupling to be performed in acidic media at pH 4. Both linkers exhibit high reactivity towards the reducing end of polysaccharides, with PDHA being slightly more reactive. Importantly, the oxime bonds formed with PDHA are more resistant to acid hydrolysis than the hydrazone bonds formed with ADH. With PDHA, it is therefore possible to couple polysaccharide blocks under non-reducing conditions. This could be advantageous for triggering copolymer dissociation through a drastic change in pH or in the presence of enzymes able to perform transimination reactions. Oximes can be reduced to amines using $NaBH_3CN$, but this takes longer than with hydrazones, due to the greater stability of oximes. Among the various coupling methods, we have demonstrated that the best approach is to couple chitosan bearing a reactive M unit to dextran end-functionalized with PDHA. This method allowed to obtain linear block copolysaccharides with molar masses higher than 50,000 g/mol. Obtaining copolymers with higher molecular weights faces challenges that are more related to physical rather than chemical factors, such as the viscosity of the reaction medium, chain entanglement, and steric hindrance. Conversely, coupling chitosan-PDHA with an excess of dextran resulted in the formation of a graft copolymer, where dextran blocks are grafted to the lateral amines of chitosan chains. This may seem surprising at first but can be explained by considering several factors: the relatively low basicity of the chitosan amines (pK_a ~ 6.5), the abundance of amines compared to PDHA, and the need of reducing conditions to obtain such grafted structures. While dextran-*grafted*-chitosan copolymers are easier to synthesize, these structures lack the cooperative complexation properties of the native chitosan compared to linear copolymers.

The solubility properties of linear chitosan-*b*-dextran copolymers are markedly different from those of typical double hydrophilic block copolymers. Specifically, chitosan-*b*-dextran copolymers are not able to self-assemble into micellar aggregates upon neutralization of the chitosan blocks. Instead, block copolymers tend to precipitate under slightly basic pH conditions due to hydrogen bonding between the amine groups of chitosan. However, the pH solubility limits of chitosan have been increased by one pH

unit, enabling these copolymers to be used under physiological conditions. Gene delivery applications are specifically targeted due to the complexing and biological properties of such copolymers.

Acknowledgments

E. Courtecuisse gratefully acknowledges the French Ministry of Higher Education and Research and the Doctoral School of Chemical Sciences of Bordeaux for the funding of her PhD fellowship.

The authors acknowledge Léna Alembik for assistance with NMR kinetics acquirement and Fiona Magliozzi for her preliminary work on this topic.

Declaration of generative AI and AI-assisted technologies in the writing process

During the preparation of this work the authors used ChatGPT only to improve language and readability. After using this tool, the authors reviewed and edited the content as needed and take full responsibility for the content of the publication.

References

Allan, G. G., & Peyron, M. (1995a). Molecular weight manipulation of chitosan I: kinetics of depolymerization by nitrous acid. *Carbohydrate Research*, *277*(2), 257-272. https://doi.org/10.1016/0008-6215(95)00207-A

Allan, G. G., & Peyron, M. (1995b). Molecular weight manipulation of chitosan II : Prediction and control of extent of depolymerization by nitrous acid. *Carbohydrate Research*, *277*(2), 273-282. https://doi.org/10.1016/0008-6215(95)00208-B

Baudendistel, O. R., Wieland, D. E., Schmidt, M. S., & Wittmann, V. (2016). Real-Time NMR Studies of Oxyamine Ligations of Reducing Carbohydrates under Equilibrium Conditions. *Chemistry – A European Journal*, *22*(48), 17359-17365. https://doi.org/10.1002/chem.201603369

Benzeval, I., Bowyer, A., & Hubble, J. (2012). The influence of degree-of-branching and molecular mass on the interaction between dextran and Concanavalin A in hydrogel preparations intended for insulin release. *European Journal of Pharmaceutics and Biopharmaceutics*, *80*(1), 143-148. https://doi.org/10.1016/j.ejpb.2011.08.009

Berth, G., Dautzenberg, H., & Peter, M. G. (1998). Physico-chemical characterization of chitosans varying in degree of acetylation. *Carbohydrate Polymers*, *36*(2), 205-216. https://doi.org/10.1016/S0144-8617(98)00029-0

Bezrodnykh, E. A., Blagodatskikh, I. V., Kulikov, S. N., Zelenikhin, P. V., Yamskov, I. A., & Tikhonov, V. E. (2018). Consequences of chitosan decomposition by nitrous acid : Approach to non-branched oligochitosan oxime. *Carbohydrate Polymers*, *195*, 551-557. https://doi.org/10.1016/j.carbpol.2018.05.007

Borch, R. F., Bernstein, M. D., & Durst, H. D. (1971). Cyanohydridoborate anion as a selective reducing agent. *Journal of the American Chemical Society*, *93*(12), 2897-2904. https://doi.org/10.1021/ja00741a013

Borchert, U., Lipprandt, U., Bilang, M., Kimpfler, A., Rank, A., Peschka-Süss, R., Schubert, R., Lindner, P., & Förster, S. (2006). PH-Induced Release from P2VP−PEO Block Copolymer Vesicles. *Langmuir*, *22*(13), 5843-5847. https://doi.org/10.1021/la060227t

Bosker, W. T. E., Ágoston, K., Cohen Stuart, M. A., Norde, W., Timmermans, J. W., & Slaghek, T. M. (2003). Synthesis and Interfacial Behavior of Polystyrene−Polysaccharide Diblock Copolymers. *Macromolecules*, *36*(6), 1982-1987. https://doi.org/10.1021/ma020925u

Breitenbach, B. B., Schmid, I., & Wich, P. R. (2017). Amphiphilic Polysaccharide Block Copolymers for pH-Responsive Micellar Nanoparticles. *Biomacromolecules*, *18*(9), 2839-2848. https://doi.org/10.1021/acs.biomac.7b00771

Butun, V., Billingham, N. C., & Armes, S. P. (1998). Unusual aggregation behavior of a novel tertiary amine methacrylate- based diblock copolymer : Formation of Micelles and reverse Micelles in aqueous solution [12]. *Journal of the American Chemical Society*, *120*(45), 11818-11819. https://doi.org/10.1021/ja982295a

Chapelle, C., David, G., Caillol, S., Negrell, C., Durand, G., Desroches le Foll, M., & Trombotto, S. (2019). Water-Soluble 2,5-Anhydro- D -mannofuranose Chain End Chitosan Oligomers of a Very Low Molecular Weight : Synthesis and Characterization. *Biomacromolecules*, *20*(12), 4353-4360. https://doi.org/10.1021/acs.biomac.9b01003

Cheetham, N. W. H., Fiala-Beer, E., & Walker, G. J. (1990). Dextran structural details from high-field proton NMR spectroscopy. *Carbohydrate Polymers*, *14*(2), 149-158. https://doi.org/10.1016/0144-8617(90)90027-P

Cheng, S., Wantuch, P. L., Kizer, M. E., Middleton, D. R., Wang, R., DiBello, M., Li, M., Wang, X., Li, X., Ramachandiran, V., Avci, F. Y., Zhang, F., Zhang, X., & Linhardt, R. J. (2019). Glycoconjugate synthesis using chemoselective ligation11Electronic supplementary information (ESI) available. See DOI: 10.1039/c9ob00270g. *Organic & Biomolecular Chemistry*, *17*(10), 2646-2650. https://doi.org/10.1039/c9ob00270g

Coudurier, M., Faivre, J., Crépet, A., Ladavière, C., Delair, T., Schatz, C., & Trombotto, S. (2020). Reducing-End Functionalization of 2,5-Anhydro-d-mannofuranose-Linked Chitooligosaccharides by Dioxyamine : Synthesis and Characterization. *Molecules*, *25*(5). https://doi.org/10.3390/molecules25051143

Delas, T., Mock-Joubert, M., Faivre, J., Hofmaier, M., Sandre, O., Dole, F., Chapel, J. P., Crépet, A., Trombotto, S., Delair, T., & Schatz, C. (2019). Effects of Chain Length of Chitosan Oligosaccharides on Solution Properties and Complexation with siRNA. *Polymers*, *11*(8). https://doi.org/10.3390/polym11081236

Dumitriu, S. (Éd.). (2004). *Polysaccharides : Structural Diversity and Functional Versatility, Second Edition* (0 éd.). CRC Press. https://doi.org/10.1201/9781420030822

Dworkin, J. P., & Miller, S. L. (2000). A kinetic estimate of the free aldehyde content of aldoses. *Carbohydrate Research*, *329*(2), 359-365. https://doi.org/10.1016/S0008-6215(00)00204-4

Edwards, J. O., & Pearson, R. G. (1962). The Factors Determining Nucleophilic Reactivities. *Journal of the American Chemical Society*, *84*(1), 16-24. https://doi.org/10.1021/ja00860a005

Gagnaire, D., & Vignon, M. (1977). Étude par 13C NMR et 1H NMR du dextrane et de ses dérivés acétylés et benzylés. *Die Makromolekulare Chemie*, *178*(8), 2321-2333. https://doi.org/10.1002/macp.1977.021780819

Gekko, K. (1981). Solution Properties of Dextran and Its Ionic Derivatives. In *Solution Properties of Polysaccharides* (Vol. 150, p. 415-438). AMERICAN CHEMICAL SOCIETY. https://doi.org/10.1021/bk-1981-0150.ch029

Gemma, E., Meyer, O., Uhrín, D., & Hulme, A. N. (2008). Enabling methodology for the end functionalisation of glycosaminoglycan oligosaccharides. *Molecular BioSystems*, *4*(6), 481-495. https://doi.org/10.1039/B801666F

Glasoe, P. K., & Long, F. A. (1960). USE OF GLASS ELECTRODES TO MEASURE ACIDITIES IN DEUTERIUM OXIDE1,2. *The Journal of Physical Chemistry*, *64*(1), 188-190. https://doi.org/10.1021/j100830a521

Gudmundsdottir, A. V., Paul, C. E., & Nitz, M. (2009). Stability studies of hydrazide and hydroxylamine-based glycoconjugates in aqueous solution. *Carbohydrate Research*, *344*(3), 278-284. https://doi.org/10.1016/j.carres.2008.11.007

Hansen, T., Vermeeren, P., Bickelhaupt, F. M., & Hamlin, T. A. (2021). Origin of the α-Effect in SN2 Reactions. *Angewandte Chemie International Edition*, *60*(38), 20840-20848. https://doi.org/10.1002/anie.202106053

Janciauskaite, U., Rakutyte, V., Miskinis, J., & Makuska, R. (2008). Synthesis and properties of chitosan-N-dextran graft copolymers. *Reactive and Functional Polymers*, *68*(3), 787-796. https://doi.org/10.1016/j.reactfunctpolym.2007.12.001

Jencks, W. P. (1964). Mechanism and Catalysis of Simple Carbonyl Group Reactions. In *Progress in Physical Organic Chemistry* (p. 63-128). https://doi.org/10.1002/9780470171813.ch2

Johnson, B. K., & Prud'homme, R. K. (2003). Mechanism for Rapid Self-Assembly of Block Copolymer Nanoparticles. *Physical Review Letters*, *91*(11), 118302. https://doi.org/10.1103/PhysRevLett.91.118302

Kalia, J., & Raines, R. T. (2008). Hydrolytic Stability of Hydrazones and Oximes. *Angewandte Chemie International Edition*, *47*(39), 7523-7526. https://doi.org/10.1002/anie.200802651

Khadem, H., & Fatiadi, A. (2000). ChemInform Abstract : Hydrazine Derivatives of Carbohydrates and Related Compounds. *Advances in Carbohydrate Chemistry and Biochemistry*, *55*, 175-263. https://doi.org/10.1016/S0065-2318(00)55006-9

Kölmel, D. K., & Kool, E. T. (2017). Oximes and Hydrazones in Bioconjugation : Mechanism and Catalysis. *Chemical Reviews*, *117*(15), 10358-10376. https://doi.org/10.1021/acs.chemrev.7b00090

Kwase, Y. A., Cochran, M., & Nitz, M. (2013). Protecting-Group-Free Glycoconjugate Synthesis : Hydrazide and Oxyamine Derivatives in N-Glycoside Formation. In *Modern Synthetic Methods in Carbohydrate Chemistry* (p. 67-96). https://doi.org/10.1002/9783527658947.ch3

Lane, C. F. (1975). Sodium cyanoborohydride—A highly selective reducing agent for organic functional groups. *Synthesis (Germany)*, *1975*(3), 135-146. https://doi.org/10.1055/s-1975-23685

Lee, E. S., Shin, H. J., Na, K., & Bae, Y. H. (2003). Poly(l-histidine)–PEG block copolymer micelles and pH-induced destabilization. *Journal of Controlled Release*, *90*(3), 363-374. https://doi.org/10.1016/S0168-3659(03)00205-0

Levy, M., & Doisy, E. A. (1928). THE EFFECT OF BORATE ON THE OXIDATION OF GLUCOSE AND OTHER SUGARS. *Journal of Biological Chemistry*, *77*(2), 733-751. https://doi.org/10.1016/S0021-9258(20)74024-X

Los, J. M., Simpson, L. B., & Wiesner, K. (1956). The Kinetics of Mutarotation of D-Glucose with Consideration of an Intermediate Free-aldehyde Form. *Journal of the American Chemical Society*, *78*(8), 1564-1568. https://doi.org/10.1021/ja01589a017

Mo, I. V., Dalheim, M. Ø., Aachmann, F. L., Schatz, C., & Christensen, B. E. (2020). 2,5-Anhydro-d-Mannose End-Functionalized Chitin Oligomers Activated by Dioxyamines or Dihydrazides as Precursors of Diblock Oligosaccharides. *Biomacromolecules*, *21*(7), 2884-2895. https://doi.org/10.1021/acs.biomac.0c00620

Moussa, A., Crépet, A., Ladavière, C., & Trombotto, S. (2019). Reducing-end "clickable" functionalizations of chitosan oligomers for the synthesis of chitosan-based diblock copolymers. *Carbohydrate Polymers*, *219*, 387-394. https://doi.org/10.1016/j.carbpol.2019.04.078

Mukherjee, S., Bapat, A. P., Hill, M. R., & Sumerlin, B. S. (2014). Oximes as reversible links in polymer chemistry : Dynamic macromolecular stars. *Polymer Chemistry*, *5*(24), 6923-6931. https://doi.org/10.1039/C4PY01282H

Munneke, S., Prevost, J. R. C., Painter, G. F., Stocker, B. L., & Timmer, M. S. M. (2015). The Rapid and Facile Synthesis of Oxyamine Linkers for the Preparation of Hydrolytically Stable Glycoconjugates. *Organic Letters*, *17*(3), 624-627. https://doi.org/10.1021/ol503634j

Novoa-Carballal, R., & Müller, A. H. E. (2012). Synthesis of polysaccharide-b-PEG block copolymers by oxime click. *Chemical Communications*, *48*(31), 3781-3783. https://doi.org/10.1039/C2CC30726J

Qin, C., Li, H., Xiao, Q., Liu, Y., Zhu, J., & Du, Y. (2006). Water-solubility of chitosan and its antimicrobial activity. *Carbohydrate Polymers*, *63*(3), 367-374. https://doi.org/10.1016/j.carbpol.2005.09.023

Ridley, B. L., Spiro, M. D., Glushka, J., Albersheim, P., Darvill, A., & Mohnen, D. (1997). A Method for Biotin Labeling of Biologically Active Oligogalacturonides Using a Chemically Stable Hydrazide Linkage. *Analytical Biochemistry*, *249*(1), 10-19. https://doi.org/10.1006/abio.1997.2165

Rief, M., Fernandez, J. M., & Gaub, H. E. (1998). Elastically Coupled Two-Level Systems as a Model for Biopolymer Extensibility. *Physical Review Letters*, *81*(21), 4764-4767. https://doi.org/10.1103/PhysRevLett.81.4764

Roy, R., Williams, R. E., & Jennings, H. J. (1984). Increase in the acyclic form of sugars in the presence of borate ions, as measured by circular dichroism. *Carbohydrate Research*, *127*(1), 165-169. https://doi.org/10.1016/0008-6215(84)85119-8

Schatz, C., & Lecommandoux, S. (2010). Polysaccharide-Containing Block Copolymers : Synthesis, Properties and Applications of an Emerging Family of Glycoconjugates. *Macromolecular Rapid Communications*, *31*(19), 1664-1684. https://doi.org/10.1002/marc.201000267

Schatz, C., Viton, C., Delair, T., Pichot, C., & Domard, A. (2003). Typical physicochemical behaviors of chitosan in aqueous solution. *Biomacromolecules*, *4*(3), 641-648. https://doi.org/10.1021/bm025724c

Shen, L., Cao, N., Tong, L., Zhang, X., Wu, G., Jiao, T., Yin, Q., Zhu, J., Pan, Y., & Li, H. (2018). Dynamic Covalent Self-Assembly Based on Oxime Condensation. *Angewandte Chemie International Edition*, *57*(50), 16486-16490. https://doi.org/10.1002/anie.201811025

Solberg, A., Mo, I. V., Aachmann, F. L., Schatz, C., & Christensen, B. E. (2021). Alginate-based diblock polymers : Preparation, characterization and Ca-induced self-assembly. *Polymer Chemistry*, *12*(38), 5412-5425. https://doi.org/10.1039/D1PY00727K

Solberg, A., Mo, I. V., Omtvedt, L. Aa., Strand, B. L., Aachmann, F. L., Schatz, C., & Christensen, B. E. (2022). Click chemistry for block polysaccharides with dihydrazide and dioxyamine

linkers—A review. *Carbohydrate Polymers*, *278*, 118840. https://doi.org/10.1016/j.carbpol.2021.118840

Sorlier, P., Denuzière, A., Viton, C., & Domard, A. (2001). Relation between the Degree of Acetylation and the Electrostatic Properties of Chitin and Chitosan. *Biomacromolecules*, *2*(3), 765-772. https://doi.org/10.1021/bm015531+

Tømmeraas, K., Köping-Höggård, M., Vårum, K. M., Christensen, B. E., Artursson, P., & Smidsrød, O. (2002). Preparation and characterisation of chitosans with oligosaccharide branches. *Carbohydrate Research*, *337*(24), 2455-2462. https://doi.org/10.1016/S0008-6215(02)00334-8

Tømmeraas, K., Strand, S. P., Christensen, B. E., Smidsrød, O., & Vårum, K. M. (2011). Preparation and characterization of branched chitosans. *Carbohydrate Polymers*, *83*(4), 1558-1564. https://doi.org/10.1016/j.carbpol.2010.10.008

Tømmeraas, K., Vårum, K. M., Christensen, B. E., & Smidsrød, O. (2001). Preparation and characterisation of oligosaccharides produced by nitrous acid depolymerisation of chitosans. *Carbohydrate Research*, *333*(2), 137-144. https://doi.org/10.1016/S0008-6215(01)00130-6

Vårum, K. M., Ottøy, M. H., & Smidsrød, O. (1994). Water-solubility of partially N-acetylated chitosans as a function of pH: effect of chemical composition and depolymerisation. *Carbohydrate Polymers*, *25*(2), 65-70. https://doi.org/10.1016/0144-8617(94)90140-6

Vikøren Mo, I., Feng, Y., Øksnes Dalheim, M., Solberg, A., Aachmann, F. L., Schatz, C., & Christensen, B. E. (2020). Activation of enzymatically produced chitooligosaccharides by dioxyamines and dihydrazides. *Carbohydrate Polymers*, *232*, 115748. https://doi.org/10.1016/j.carbpol.2019.115748

Volokhova, A. S., Edgar, K. J., & Matson, J. B. (2020). Polysaccharide-containing block copolymers : Synthesis and applications. *Materials Chemistry Frontiers*, *4*(1), 99-112. https://doi.org/10.1039/C9QM00481E

Wanjun, T., Cunxin, W., & Donghua, C. (2005). Kinetic studies on the pyrolysis of chitin and chitosan. *Polymer Degradation and Stability*, *87*(3), 389-394. https://doi.org/10.1016/j.polymdegradstab.2004.08.006

Weinhold, M. X., & Thöming, J. (2011). On conformational analysis of chitosan. *Carbohydrate Polymers*, *84*(4), 1237-1243. https://doi.org/10.1016/j.carbpol.2011.01.011

White, J. A., & Deen, W. M. (2002). Agarose-Dextran Gels as Synthetic Analogs of Glomerular Basement Membrane : Water Permeability. *Biophysical Journal*, *82*(4), 2081-2089. https://doi.org/10.1016/S0006-3495(02)75555-0

Yalpani, M., & Hall, L. D. (1984). Some chemical and analytical aspects of polysaccharide modifications. III. Formation of branched-chain, soluble chitosan derivatives. *Macromolecules*, *17*(3), 272-281. https://doi.org/10.1021/ma00133a003

Graphical abstract

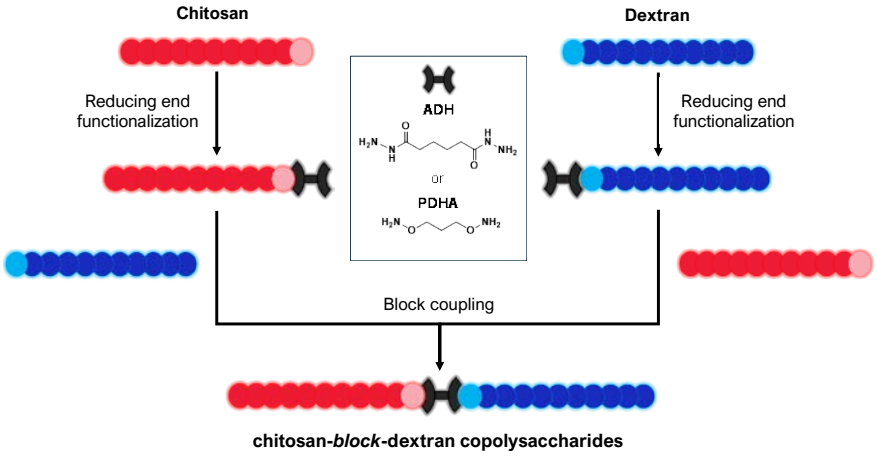

Supporting information

Synthesis of linear chitosan-*block*-dextran copolysaccharides with dihydrazide and dioxyamine linkers

Elise Courtecuisse, Sylvain Bourasseau, Bjørn E. Christensen, Christophe Schatz

Table of contents

S1. Chitosan depolymerization

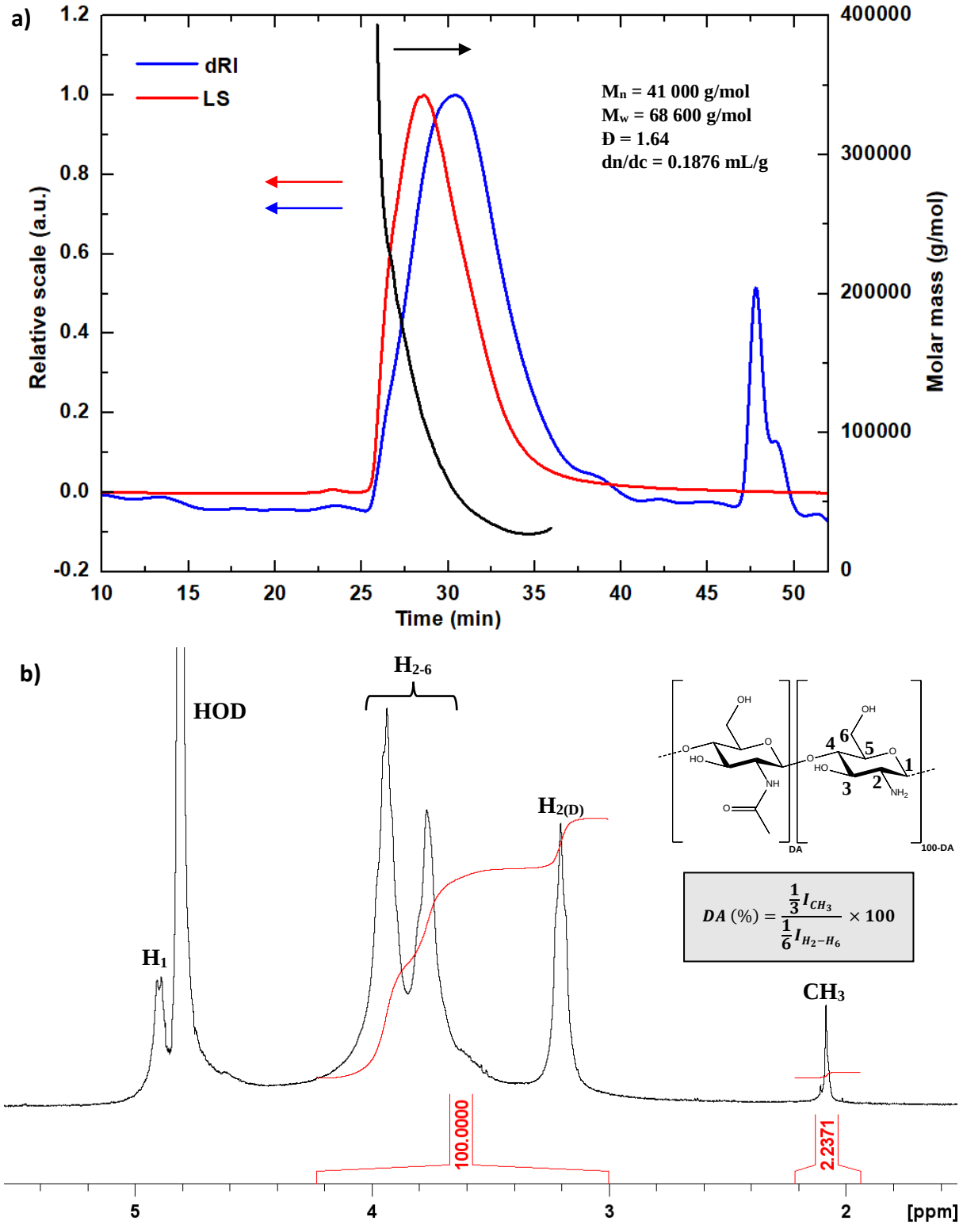

Figure S1. a) SEC-MALS analysis of the starting chitosan from Stellar Biosol (batch 144/090605) in acetate buffer (0.2 M AcOH/0.15 M AcONa, pH 4.5) with dual light scattering (red) and differential refractive index (blue) detection. b) ^{1}H-NMR analysis of the chitosan at 10 g/L in D_2O + DCl (pH = 4). The degree of acetylation was determined according to the formula of Hirai.[1]

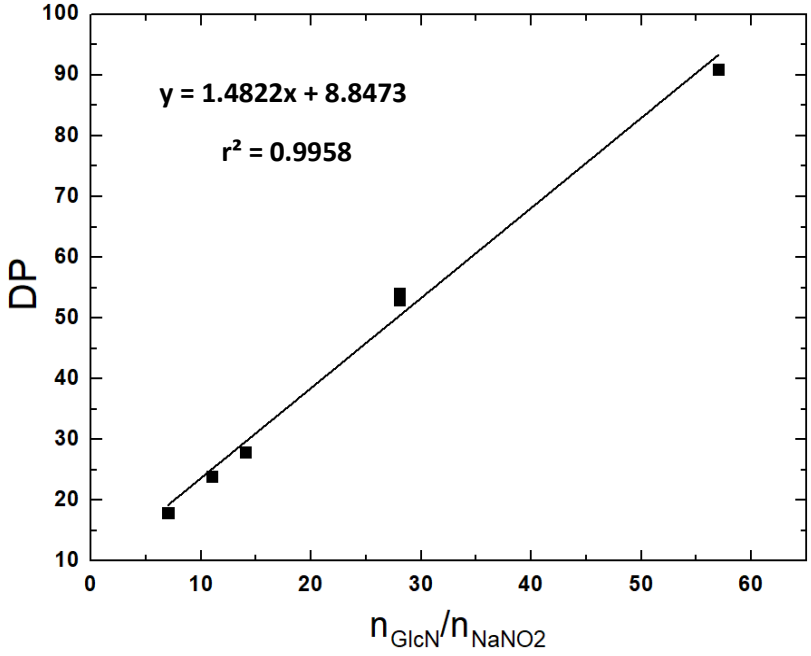

Figure S2. Degree of polymerization (DP) of chitosans obtained by NMR as a function of the initial GlcN/$NaNO_2$ molar ratio.

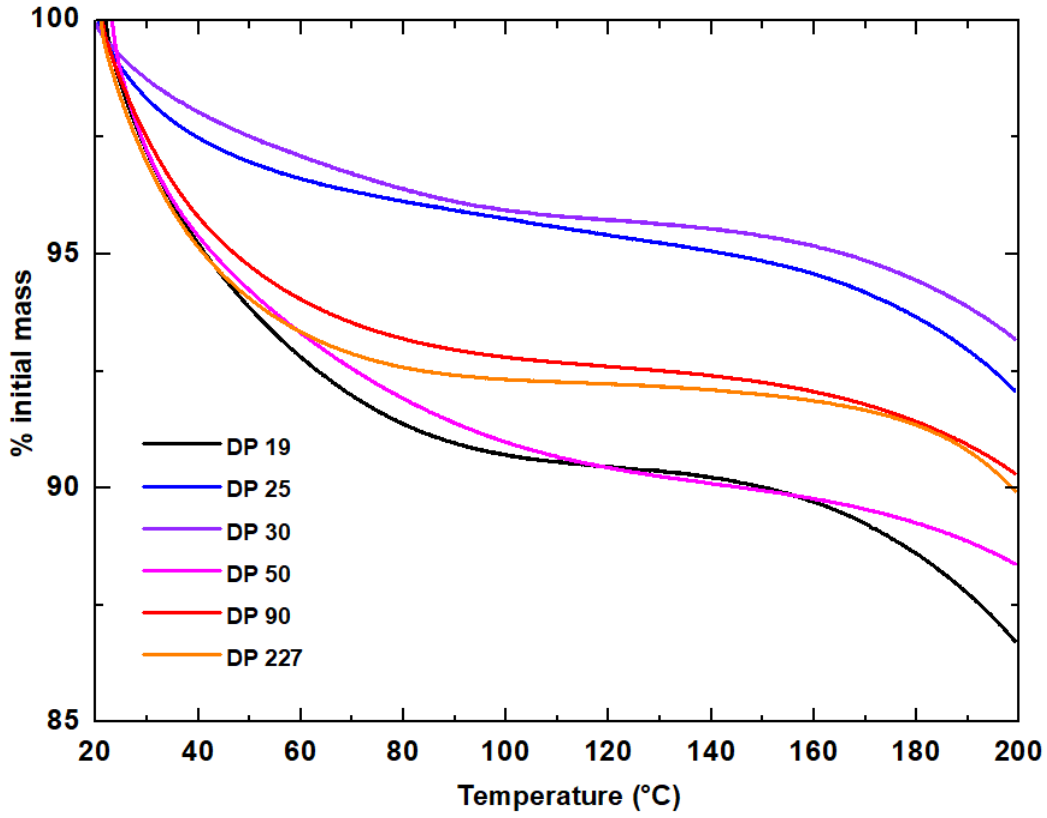

Figure S3. Thermogravimetric analysis of chitosans varying in DP at 2°C/min under N_2 atmosphere.

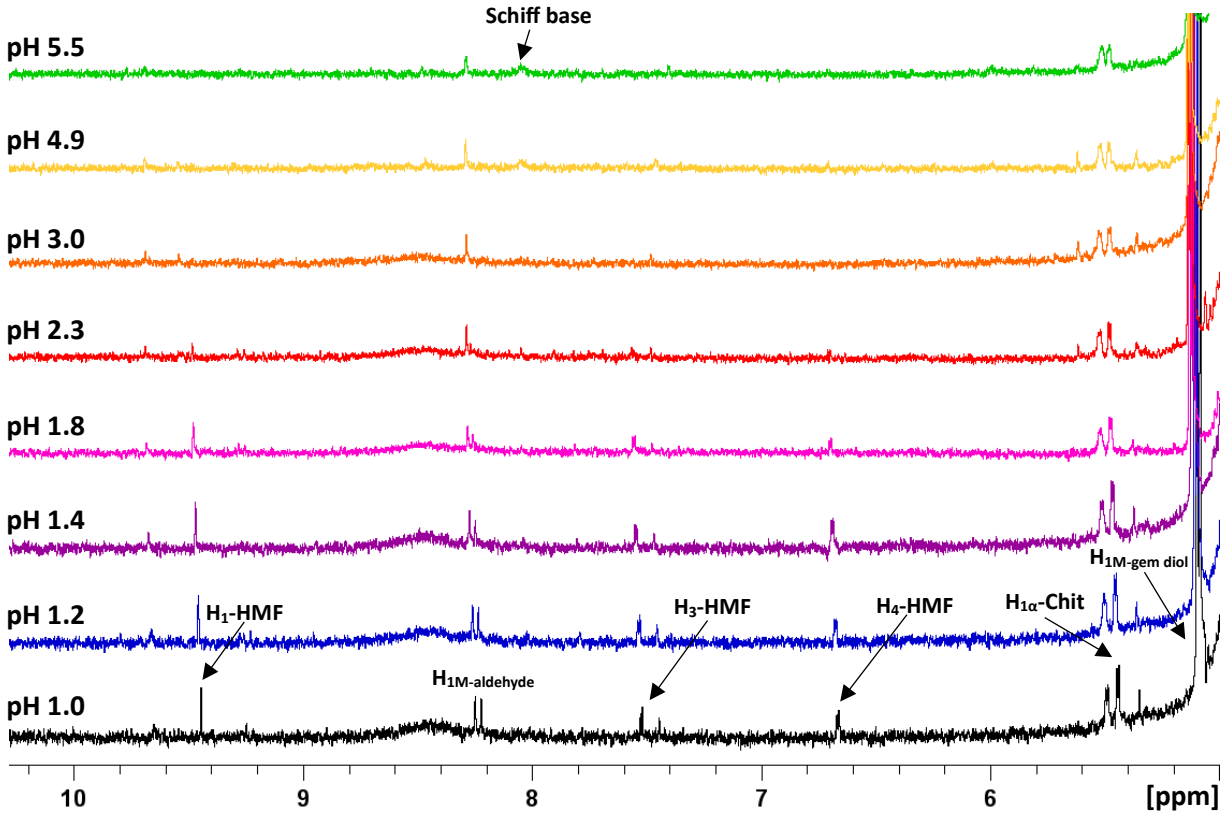

Figure S4. ^{1}H-NMR analysis of chitosan at different pHs. A solution of $Chit_{25}$ at 10 g/L in D_2O was acidified by adding increasing amounts of DCl. Peaks of low intensity at ~8.2 ppm were attributed to the aldehyde groups of the M units, which can also be present in small quantities in their free form.[3]

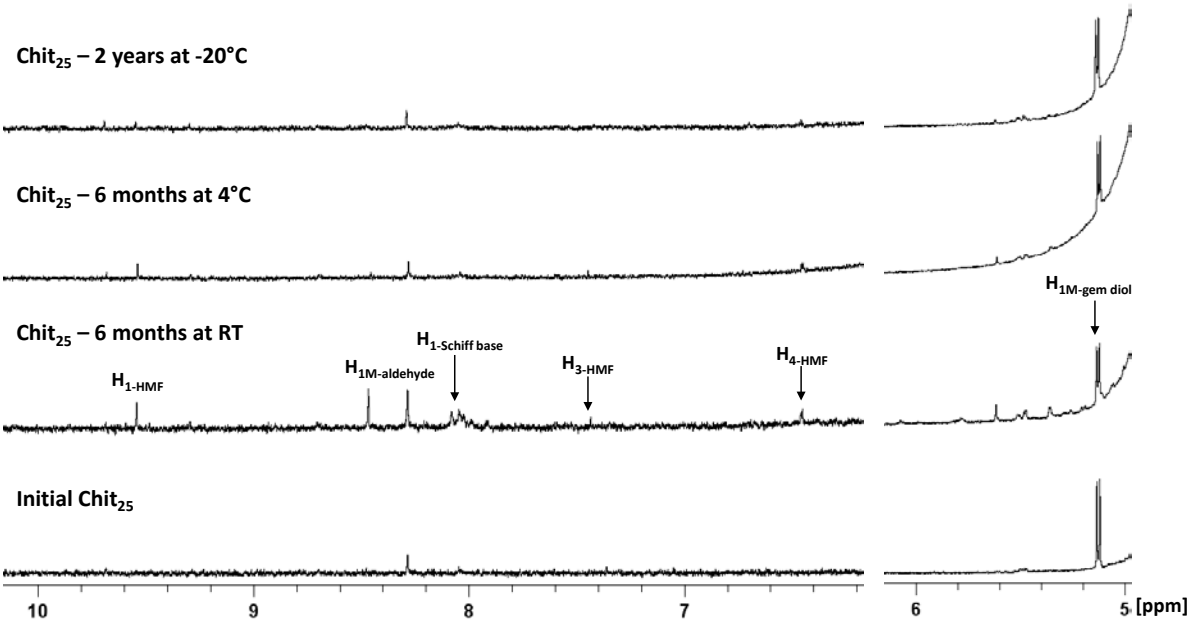

Figure S5. ^{1}H-NMR analysis of freeze-dried $Chit_{25}$ stored under various conditions of time and temperature. $Chit_{25}$ was dissolved at 10 g/L in D_2O and the solution adjusted to pH 4.5.

S2. Dimerization theoretical calculations

Statistical calculations were done to determine the percentage of dimers obtained as a function of the linker equivalents.[4] These calculations assume that the two terminal units of the diamino linkers have the same reactivities.

$[PS]_0$: Initial molar concentration of polysaccharide (chitosan or dextran)

$[L]_0$: Initial molar concentration of diamino linker (ADH or PDHA)

$[\text{-}NH_2]_0$: Initial molar concentration of terminal amine

a is defined as the initial molar excess of linker relative to the polysaccharide.

Hence: $[L]_0 = a[PS]_0$.

Since we treat each terminal amine as a separate and independent reactant we may further write:

$[\text{-}NH_2]_0 = 2[L]_0 = 2a[PS]_0$.

Let *b* be defined as the fraction of oligosaccharide that has become substituted. *b* corresponds directly from the equilibrium yields listed in Table S3. Hence, $b[PS]_0$ becomes the molar concentration of linked polysaccharide, which must necessarily equal the molar concentration of linked amine. The fraction of substituted amines (*p*) thus becomes:

$p = b[PS]_0/2a[PS]_0 = b/2a$.

Therefore, *p* is a simple function of the reaction yield (*b*) and the initial molar excess of linker (*a*). For a statistical distribution, we may equal fractions and probabilities.

Double substitution. The probability that both ends of the linker are substituted: (f_{DS}): p^2

No substitution. The probability that none of the ends are substituted (f_{NS}): $(1 - p)^2$

Monosubstitution. The probability that one of the ends is substituted (f_{MS}): $1 - p^2 - (1 - p)^2 = 2p(1\text{-}p)$

Assuming a full conversion yield of the reducing end of polysaccharide (b=1), the fraction of double substituted (f_{DS}), non-substituted (f_{NS}) and mono-substituted (f_{MS}) conjugate are given for various amounts of linker (*a*) (Table S3). Then, the effective fraction of dimerized polysaccharide blocks corresponds to $f_{DS}/(f_{DS} + f_{MS})$.

Table S1. Probabilities of the various types of substitution of a polysaccharide block by a diamino linker and the corresponding fractions of dimerized polysaccharides.

Experimental parameters	PS + 0.5eq. linker	PS + 1eq. linker	PS + 2eq. linker	PS + 3eq. linker	PS + 10eq. linker	PS + 20eq. linker	PS + 50eq. linker
a (excess linker)	0.5	1	2	3	10	20	50
b (yield)	1	1	1	1	1	1	1
p	1	0.50	0.25	0.17	0.050	0.025	0.010
f_{DS}	1	0.25	0.063	0.028	0.0025	0.00063	0.00010
f_{NS}	0	0.25	0.56	0.69	0.90	0.95	0.98
f_{MS}	0	0.50	0.38	0.28	0.095	0.049	0.020
% dimerization	100	33.3	14.3	9.1	2.6	1.3	0.5

S3. Kinetics of chitosan and dextran end-functionalization with ADH/PDHA and diaminobutane

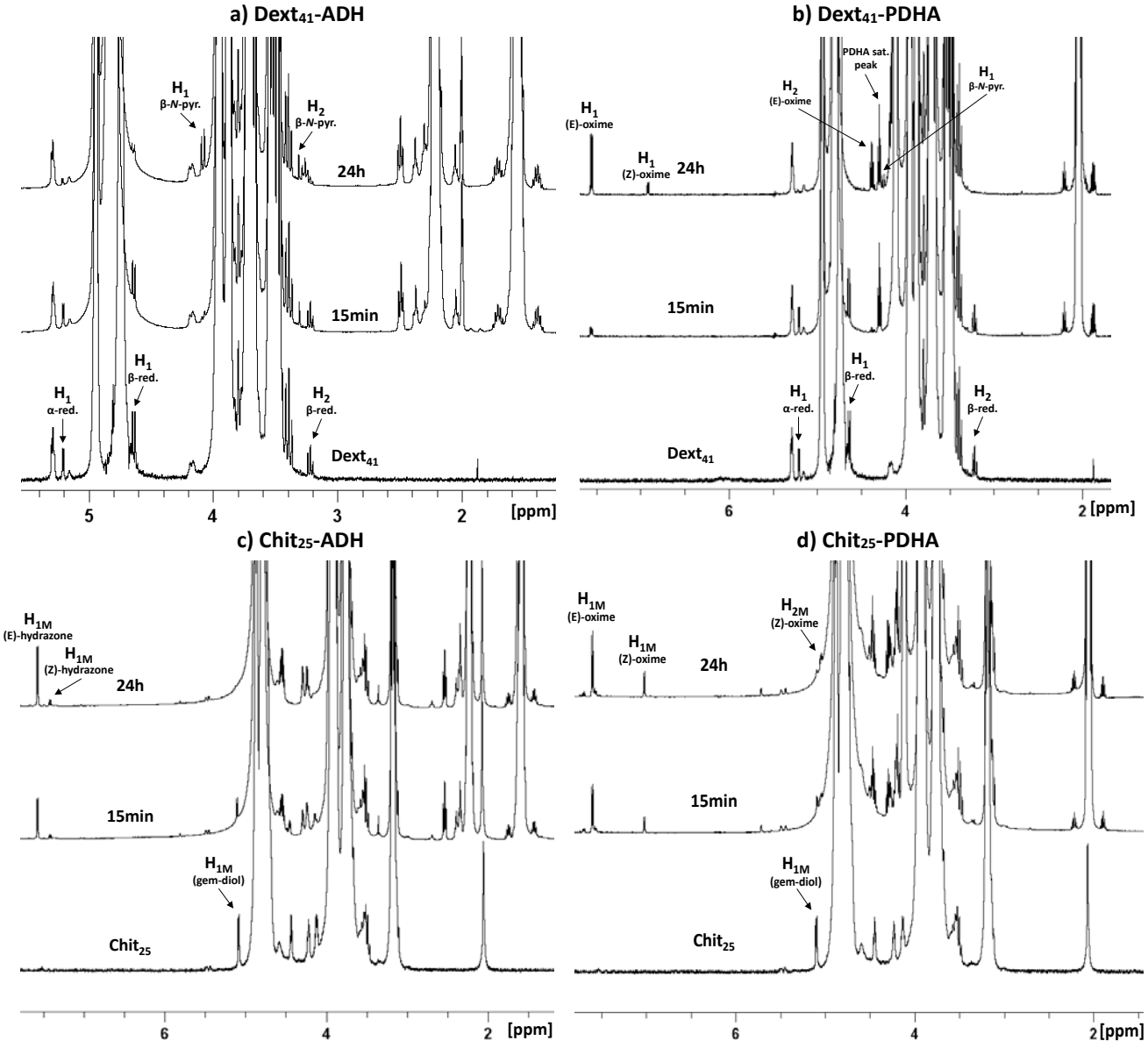

Figure S6. ^{1}H-NMR analysis of the reaction mixtures of $Dext_{41}$ and $Chit_{25}$ with 20 equivalents of ADH and PDHA under non-reductive conditions after 15 minutes and 24 hours of reaction. a) $Dext_{41}$-ADH, b) $Dext_{41}$-PDHA, c) $Chit_{25}$-ADH and d) $Chit_{25}$-PDHA. Reactions were performed at pH 4.0 (deuterated acetate buffer for dextran and D_2O + DCl for chitosan). NMR spectra of $Dext_{41}$ and $Chit_{25}$ are shown as references.

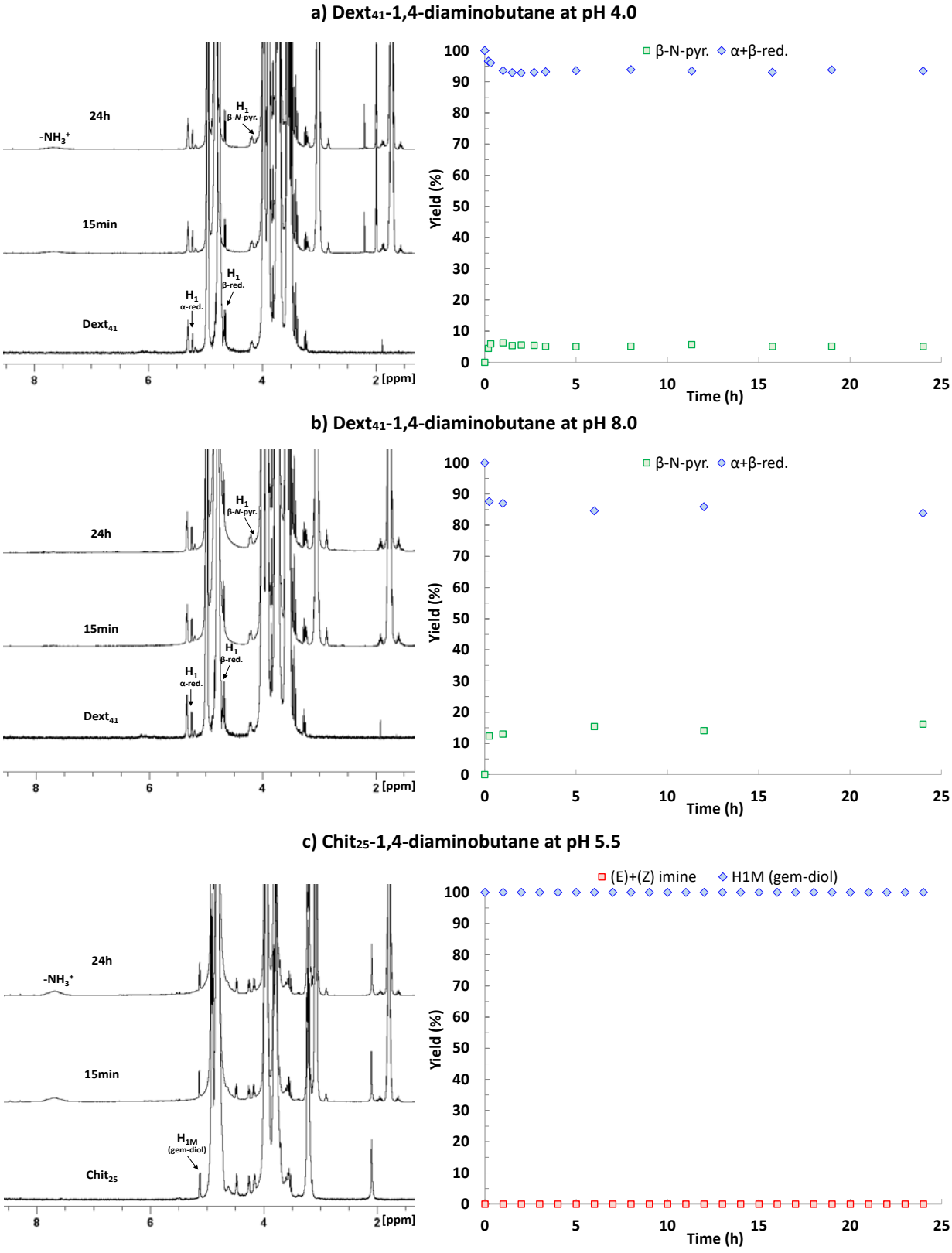

Figure S7. (Left) ^{1}H-NMR analysis of the reaction mixtures of $Dext_{41}$ and $Chit_{25}$ with 20 equivalents of 1,4-diaminobutane under non-reductive conditions after 15 minutes and 24 hours of reaction. a) $Dext_{41}$-diaminobutane at pH 4.0, b) $Dext_{41}$-diaminobutane at pH 8.0, c) $Chit_{25}$-diaminobutane at pH 5.5. NMR spectra of $Dext_{41}$ and $Chit_{25}$ are shown as references. (Right) Time course NMR analysis of the conjugation reactions of $Dext_{41}$ and $Chit_{25}$ with 1,4-diaminobutane at various pHs (pH 4.0: deuterated acetate buffer, pH 5.5: D_2O + DCl, pH 8.0: D_2O + DCl).

Table S2. Reaction yields and kinetic parameters derived from time course NMR analysis for the conjugation of $Chit_{25}$ and $Dext_{41}$ with 20 equivalents of 1,4-diaminobutane at various pHs.

Conjugate	pH	$t_{0.5}$ (h)	$t_{0.9}$ (h)	Yield (%)
$Dext_{41}$-1,4-diaminobutane	4.0	0.06	0.21	5
$Dext_{41}$-1,4-diaminobutane	8.0	0.09	0.30	15
$Chit_{25}$-1,4-diaminobutane	5.5	-	-	0

S4. pH-stability of non-reduced chitosan and dextran conjugates

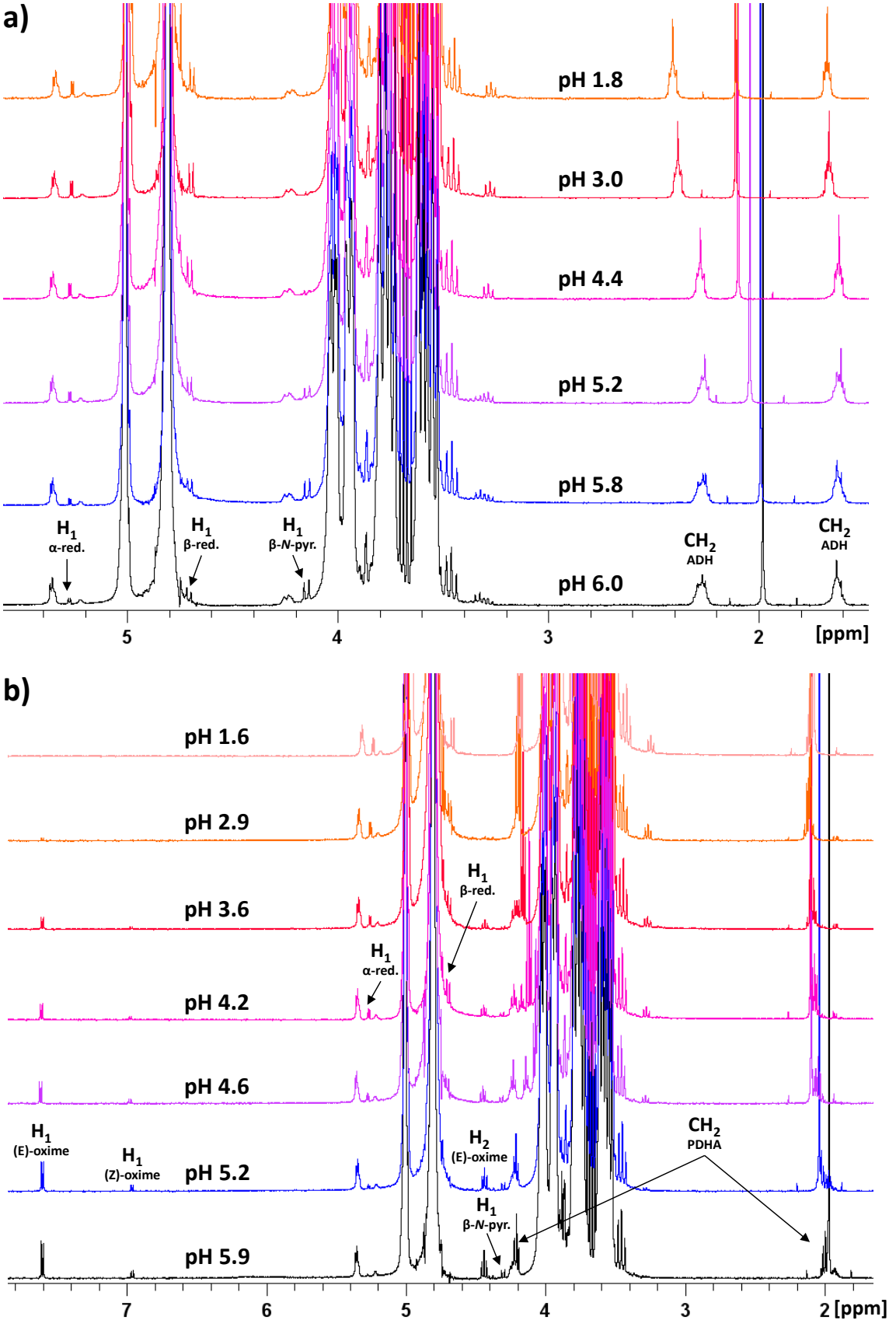

Figure S8. ^{1}H-NMR analysis of non-reduced conjugates at different pHs: a) $Dext_{41}$-ADH and b) $Dext_{41}$-PDHA. Solutions were prepared at 10 g/L in D_2O and the pH adjusted with DCl 1.17M.

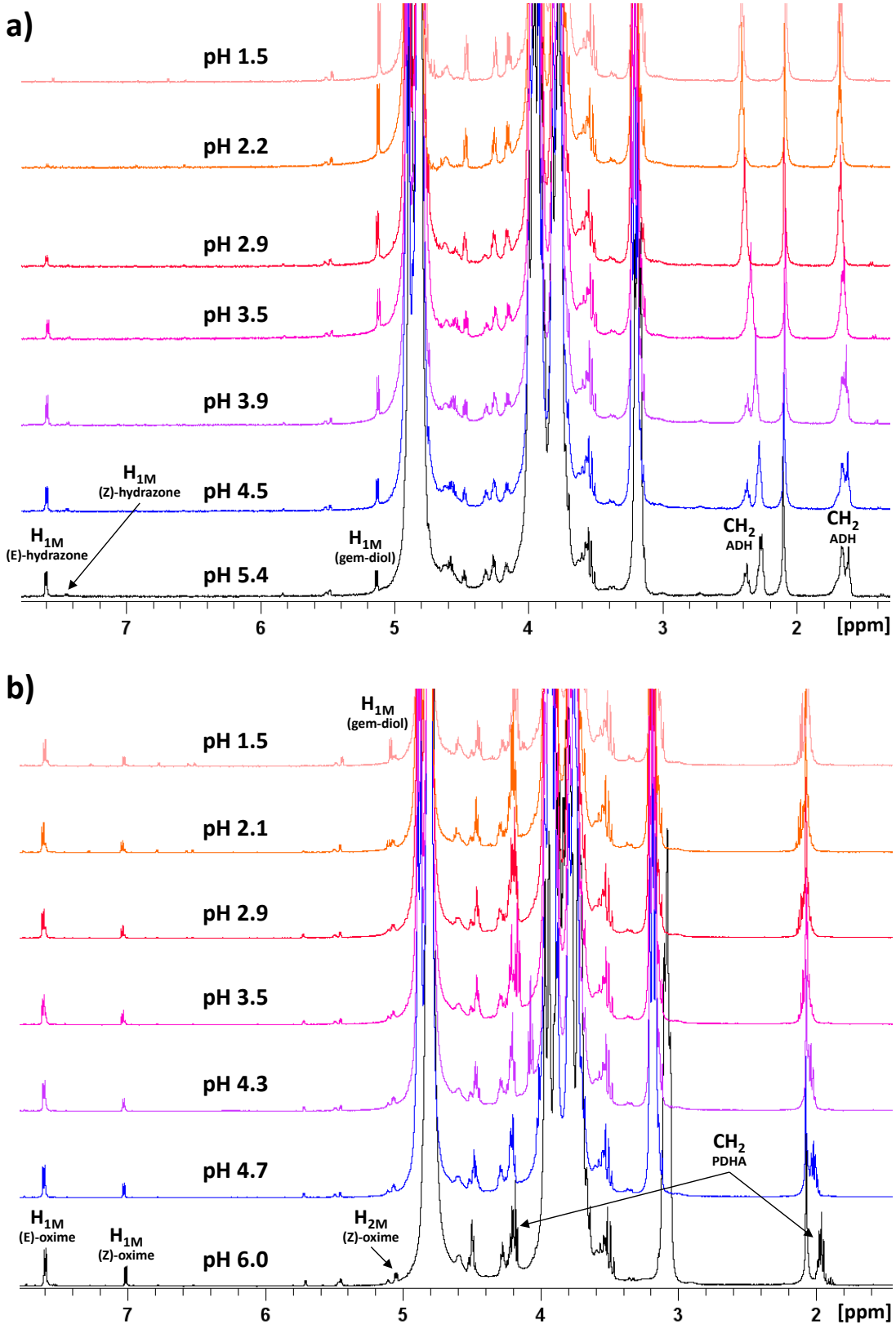

Figure S9. ^{1}H-NMR analysis of non-reduced conjugates at different pHs: a) $Chit_{25}$-ADH and b) $Chit_{25}$-PDHA. Solutions were prepared at 10 g/L in D_2O and the pH adjusted with DCl 1.17M.

S5. Conjugate reduction with $NaBH_3CN$

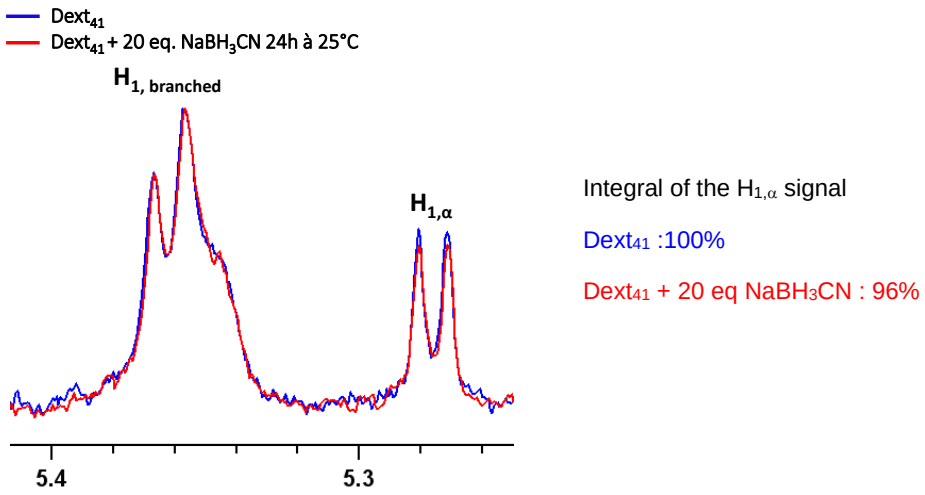

Figure S10. ^{1}H-NMR analysis of $Dext_{41}$ in D_2O after 24 hours of reaction with 20 eq of $NaBH_3CN$ in acetate buffer pH 4.0 at 25°C. Spectra were zoomed in the region corresponding to the α(1→3) protons of the branched units (unchanged after reduction) and the $H_{1,\alpha}$ protons of the reducing end.

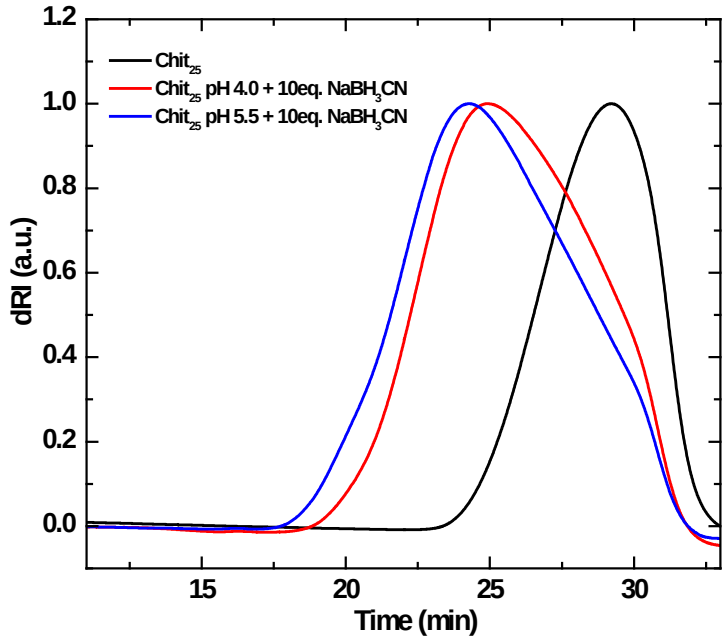

Figure S11. SEC traces (dRI signal) of $Chit_{25}$ after addition of 10 equivalents of $NaBH_3CN$. The reduction was performed for 24h at 25°C at two pH values: pH 4.0 (acetate buffer) and pH 5.5 (D_2O + DCl). The reaction mixtures were directly injected in SEC after dilution with the acetate buffer used as eluent (0.2 M AcOH/0.15 M AcONa, pH 4.5). Each chromatogram is scaled against its own magnitude.

Table S3. SEC-MALS characterization of branched chitosan structures obtained by addition of $NaBH_3CN$.

Name	M_n (g/mol)	M_w (g/mol)	Đ
$Chit_{25}$	3700	4700	1.26
$Chit_{25}$ – pH 4.0 – Ac. buffer - 10 eq. $NaBH_3CN$	9700	17200	1.78
$Chit_{25}$ – pH 5.5 – D_2O - 10 eq. $NaBH_3CN$	12900	23800	1.85

Table S4. Final pH values in the reaction mixtures for the conjugation of $Dext_{41}$ and $Chit_{25}$ with ADH/PDHA at 25°C in the presence of various amounts of $NaBH_3CN$.

Polysaccharide	Linker	Solvent	$NaBH_3CN$	Initial pH	Reduction time	Final pH
$Dext_{41}$	20 eq. ADH	acetate buffer	1x10 eq.	4.0	12 h	4.1
$Dext_{41}$	20 eq. PDHA	acetate buffer	2x10 eq.	4.0	24 h	4.0
$Chit_{25}$	20 eq. ADH	water	1x10 eq.	4.0	12 h	5.2
$Chit_{25}$	20 eq. PDHA	water	3x10 eq.	4.0	36 h	4.2

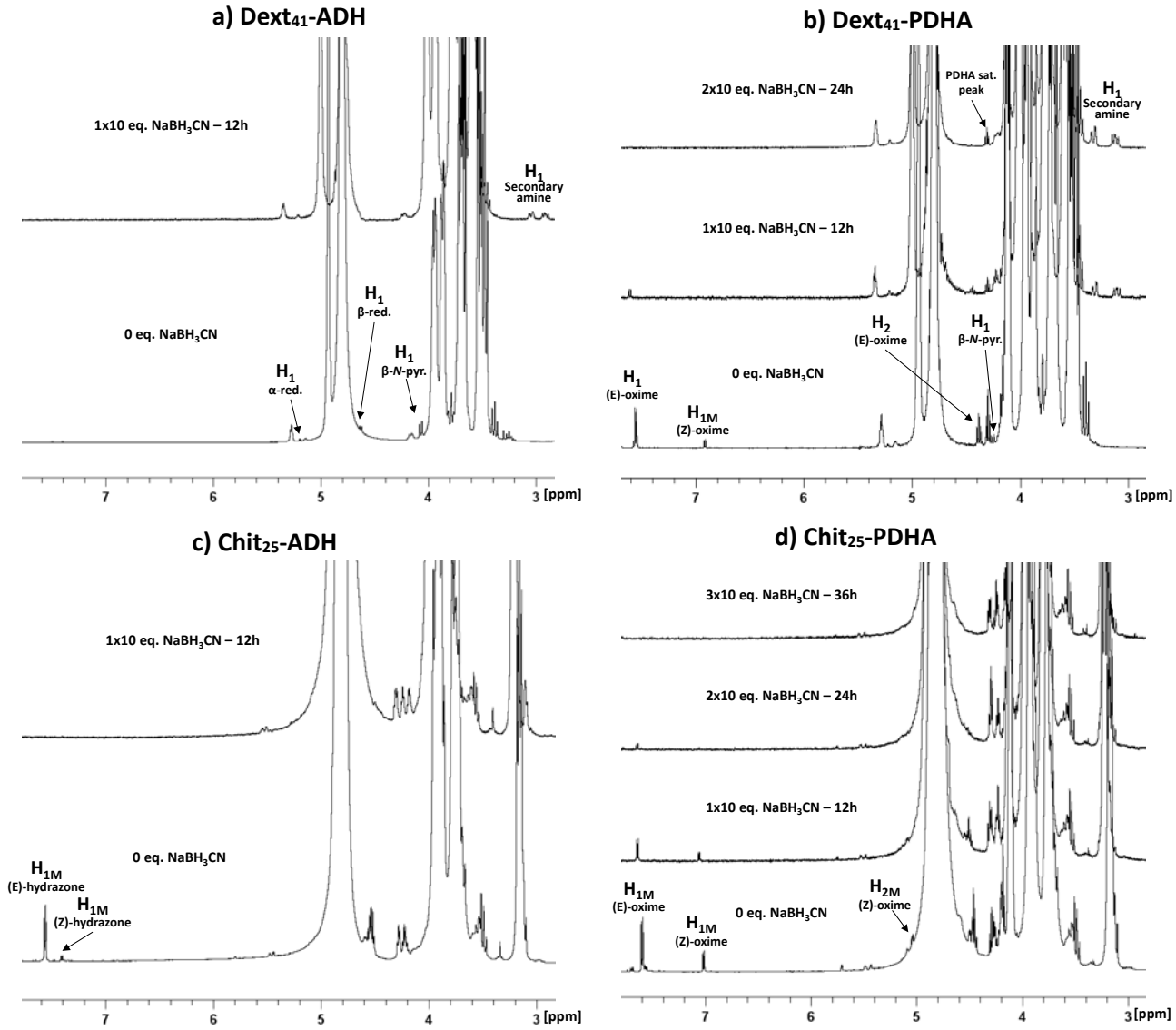

Figure S12. ^{1}H-NMR analysis of the reaction mixtures before and after each addition of $NaBH_3CN$: a) $Dext_{41}$-ADH, b) $Dext_{41}$-PDHA, c) $Chit_{25}$-ADH and d) $Chit_{25}$-PDHA. Multiple additions were performed at 12-hour intervals.

a)

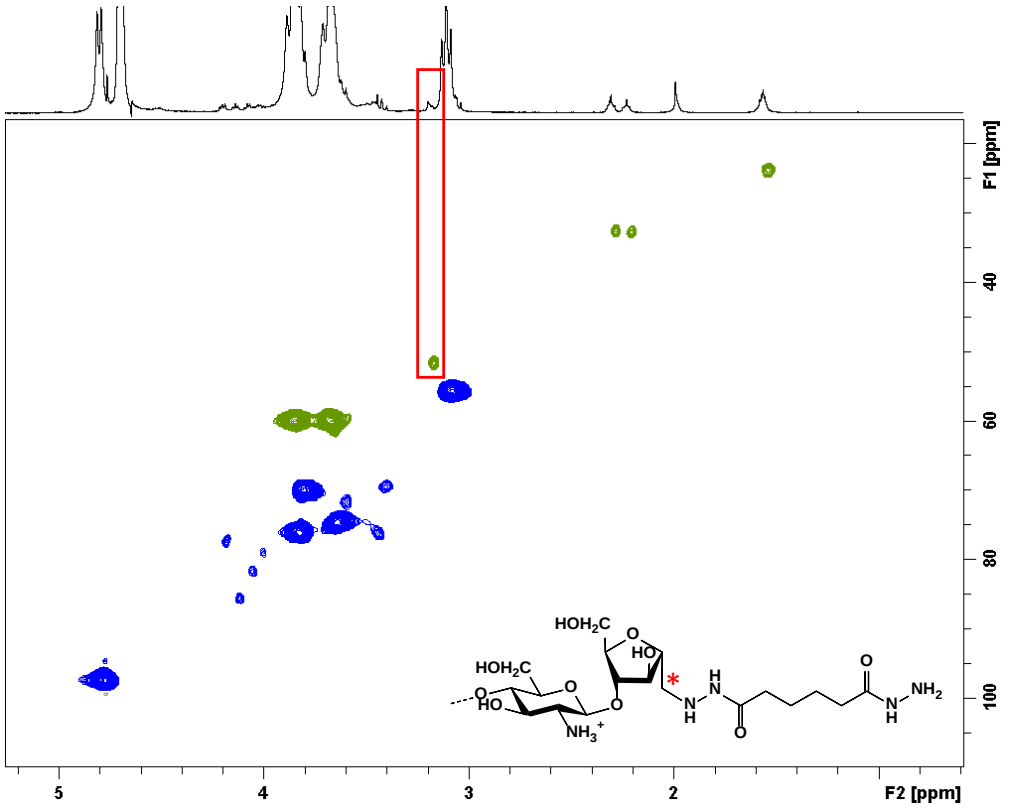
F1 [ppm]
40
60
80
100
5
4
3
2
F2 [ppm]
HOH2C
O
HO
HOH2C
O
HO
O
NH3+
*
H
N
N
H
O
O
N
H
NH2

b)

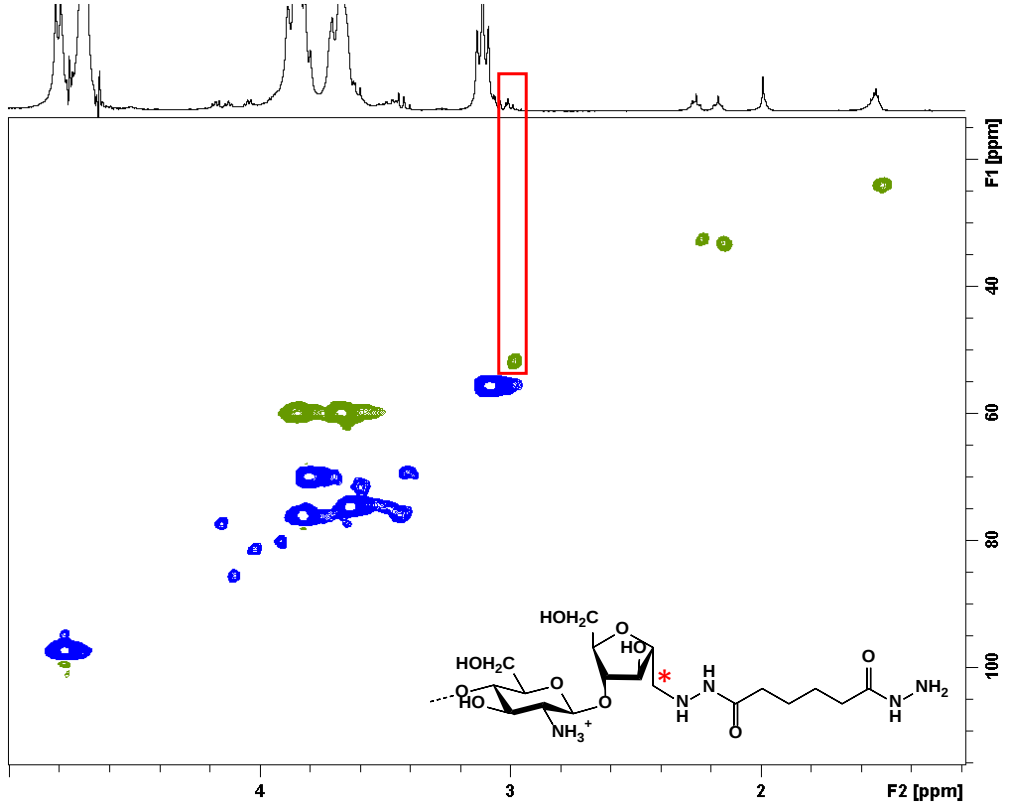
F1 [ppm]
40
60
80
100
4
3
2
F2 [ppm]
HOH2C
O
HO
HOH2C
O
HO
O
NH3+
*
H
N
N
H
O
O
N
H
NH2

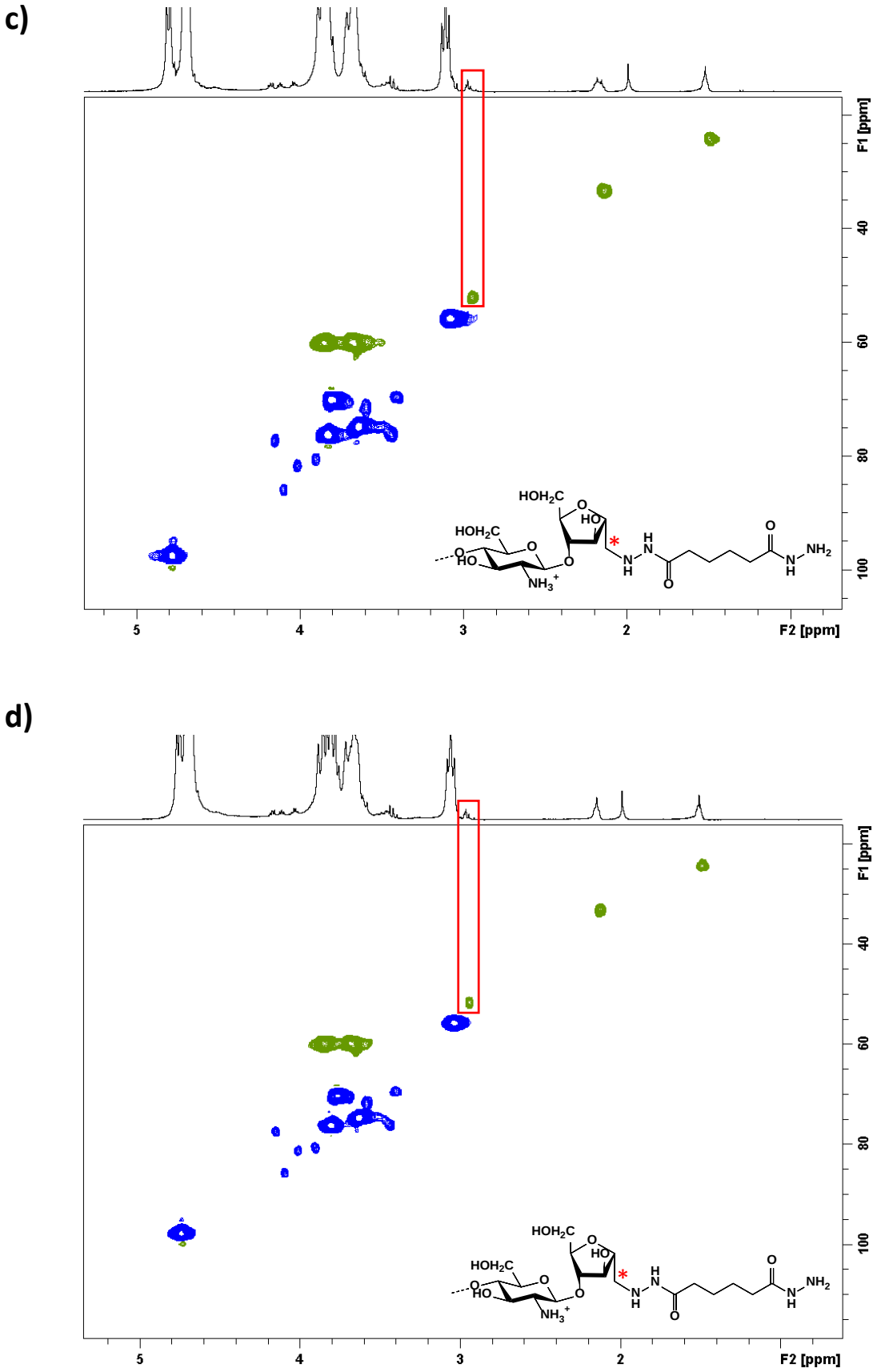

Figure S13. 2D HSQC-NMR analysis of the reduced $Chit_{25}$-ADH conjugate performed at various pHs a) pH 2.0, b) pH 3.0, c) pH 4.0 and d) pH 5.5. CH_2 groups are represented in green and CH/CH_3 groups in blue.

To ensure the absence of dimerization reactions with ADH/PDHA, SEC-MALS analysis of reduced conjugates was performed by directly injecting the reaction mixtures after dilution with the SEC eluent, thereby avoiding any increase in molar mass that could result from purification by precipitation (Figure S14 and Table S5). Dextran conjugates were analyzed in phosphate buffer at pH 9.0 to avoid protonation of ADH/PDHA end groups which can occur in acetate buffer at pH 4.5. For chitosan conjugates, acetate buffer was necessary to ensure good solubility conditions of the polymer. The increase in molar mass of dextran conjugates compared to the initial dextran was reasonably low, consistent with the low molar mass of ADH/PDHA end-group. The mass recoveries were higher than 70%. For chitosan, a significant increase in molar mass was observed for both conjugates, but likely for different reasons. For $Chit_{25}$-ADH, the high mass recovery indicates the absence of interaction with the column, thus excluding any possible interaction of the polymer with the stationary phase at pH 4.5. Under these conditions, the increase of the molar mass must be related to self-branching reactions, as described in the text. For $Chit_{25}$-PDHA, self-branching reactions are minimized due to the better stability of the oxime linkage. Therefore, the increase in molar mass must be related to the interaction of PDHA groups with the column, as evidenced by the low value of mass recovery. Electrostatic interaction involving protonated PDHA groups and residual carboxylated groups of the stationary phase (hydroxylated polymethacrylate) is suspected due to the pK_a value of PDHA (4.1), which is close to the pH of the buffer (4.5). Under these conditions, low molar mass fractions of $Chit_{25}$-PDHA conjugates are more prone to interact with the column, leading to the observed increase in the average molar mass of the conjugate.

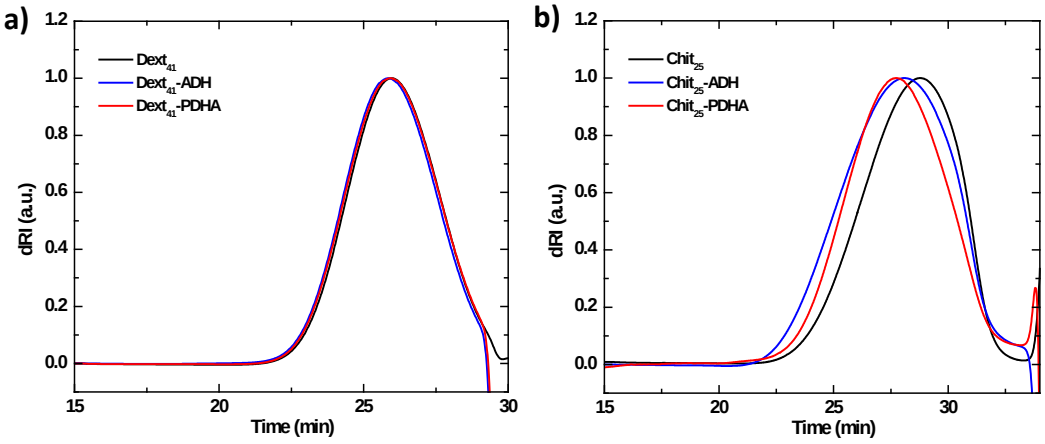

Figure S14. SEC traces (dRI signal) of reduced conjugates. a) $Dext_{41}$-ADH/PDHA in phosphate buffer pH 9.0. b) $Chit_{25}$-ADH/PDHA in acetate buffer pH 4.5.

Table S5. SEC-MALS characterization of reduced $Dext_{41}$-ADH/PDHA and $Chit_{25}$-ADH/PDHA conjugates.[a]

Name	Buffer	M_n (g/mol)	M_w (g/mol)	Đ	dn/dc (mL/g)	Mass recovery (%)
$Dext_{41}$	phosphate pH 9.0	8400	10300	1.23	0.1354	84
$Dext_{41}$-ADH	phosphate pH 9.0	8700	10500	1.21	0.1351	73
$Dext_{41}$-PDHA	phosphate pH 9.0	8800	10700	1.22	0.1358	74
$Chit_{25}$	acetate pH 4.5	4300	5600	1.31	0.1912	97
$Chit_{25}$-ADH	acetate pH 4.5	5700	7600	1.34	0.1860	86
$Chit_{25}$-PDHA	acetate pH 4.5	5600	7100	1.28	0.1723	39

[a] Direct injection of the reaction mixtures after dilution with the SEC eluent

S6. NMR characterization of the block copolysaccharides before purification

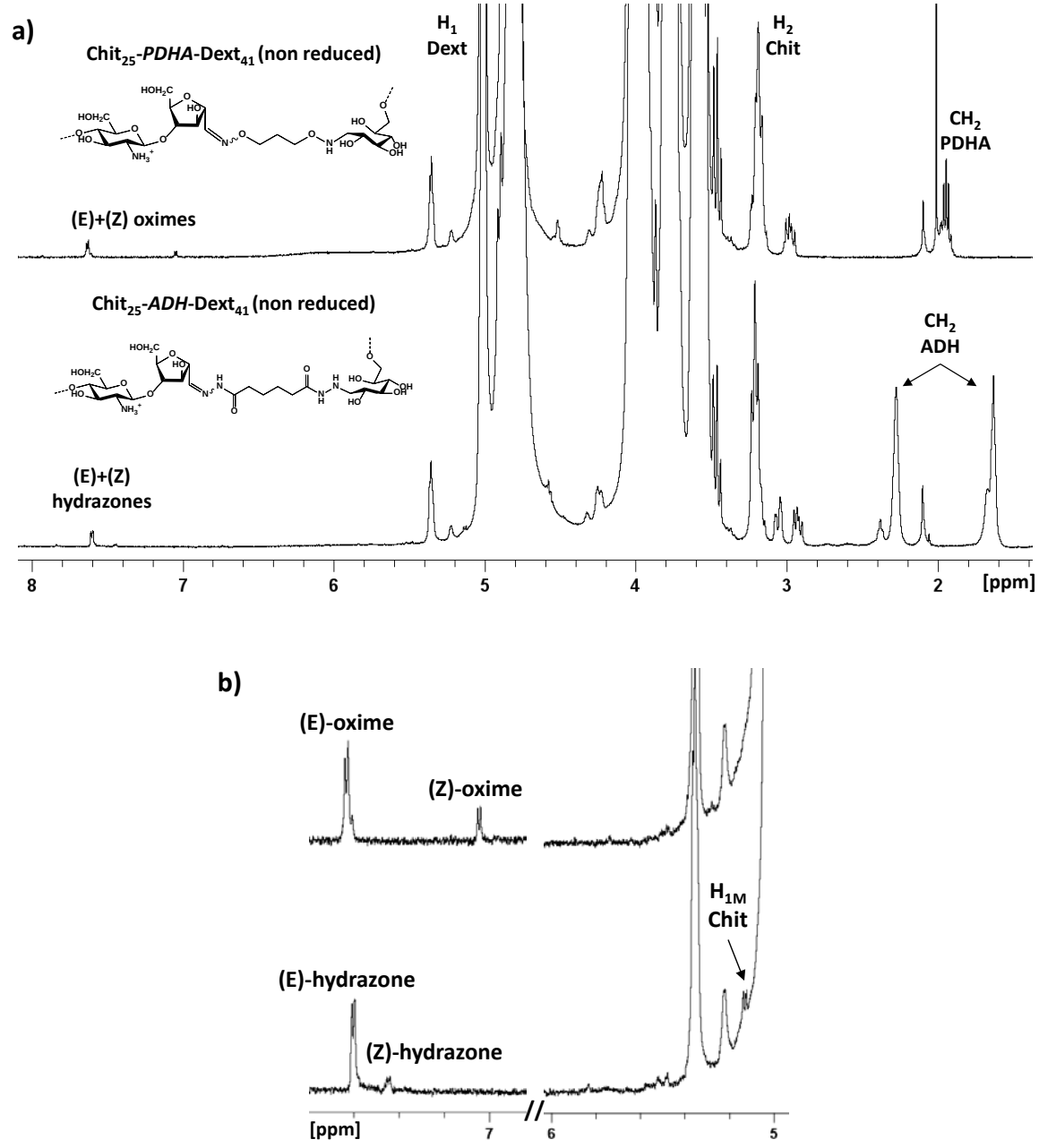

Figure S15. a) ^{1}H-NMR spectra of the reaction mixtures of $Chit_{25}$ with 3 eq. of $Dext_{41}$-ADH and $Dext_{41}$-PDHA, both under their reduced forms, after 4h of reaction. b) NMR signals of oxime and hydrazone protons (left) and residual gem-diol (right).

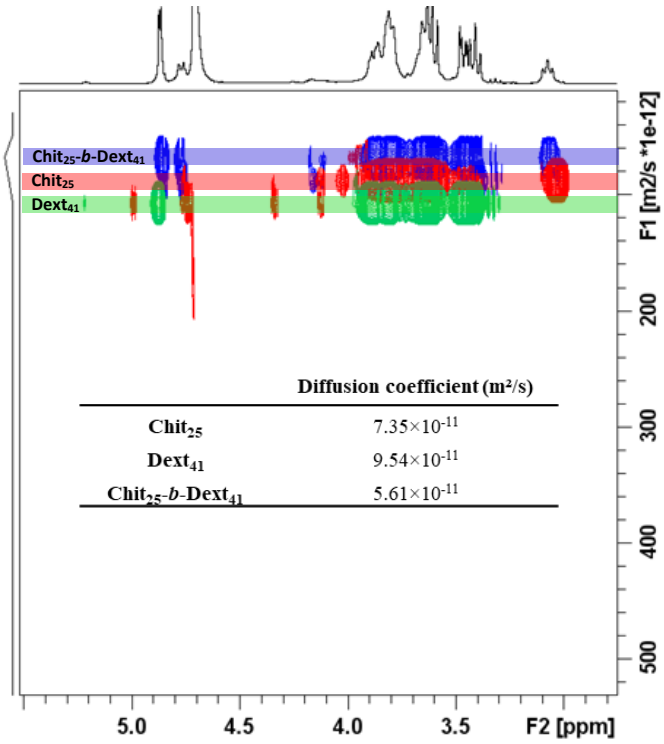

Figure S16. ^{1}H DOSY NMR spectra and diffusion coefficient values of non-purified Chit$_{25}$-*b*-Dext$_{41}$ and its precursors.

S7. Purification of the block copolysaccharides

Semi-preparative SEC was used to isolate fractions containing the $Chit_{25}$-*PDHA*-$Dext_{41}$ copolymer from those containing free chitosan. The first step was to optimize parameters such as polymer concentration, injected volume and flow rate, one by one. (Figure S15).

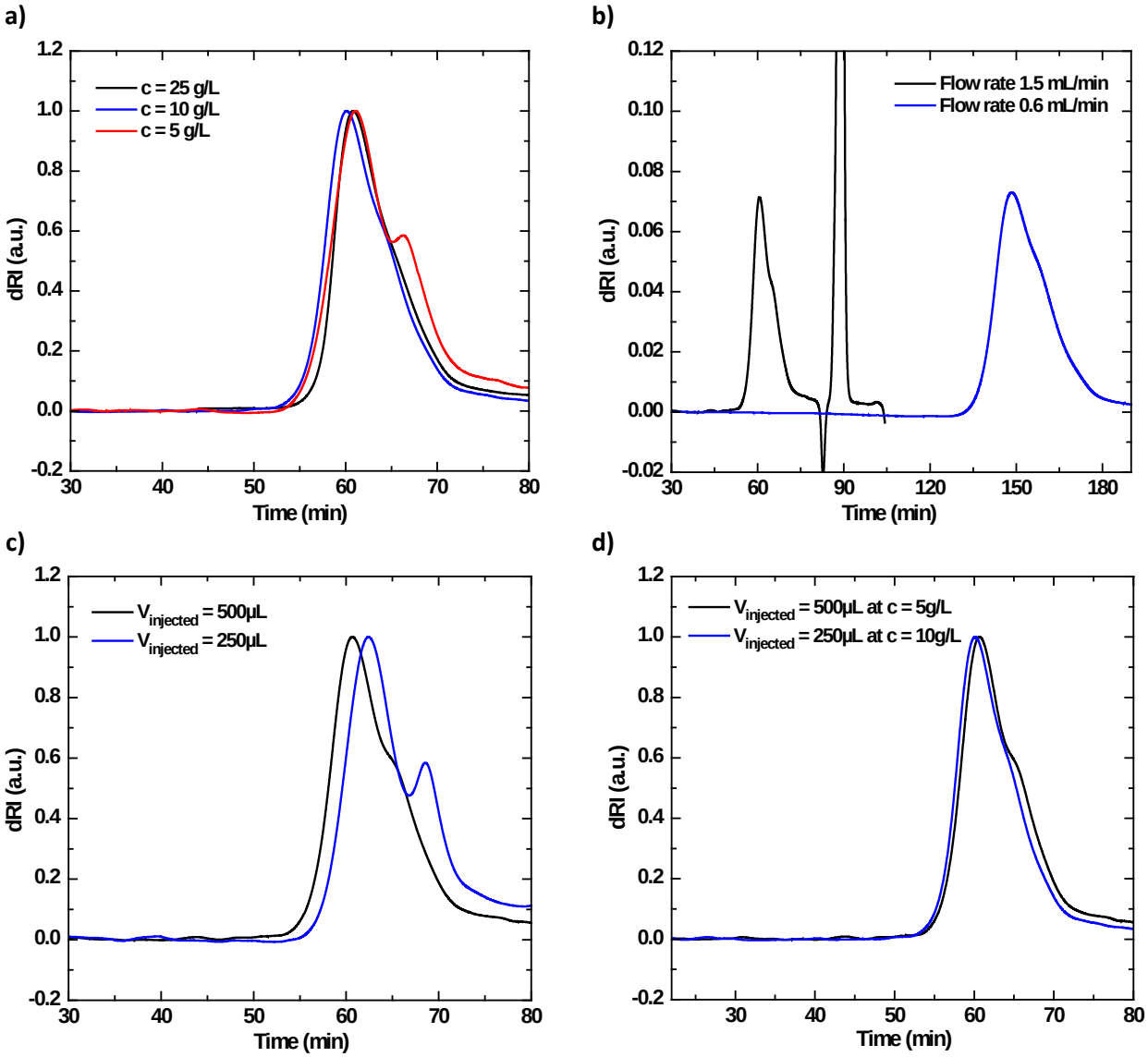

Figure S17. Optimization of the parameters for the semi-preparative separation of $Chit_{25}$-*PDHA*-$Dext_{41}$ performed in 0.2 M acetate buffer AcOH/0.15 M AcONa - pH 4.5. a) influence of the polymer concentration ($V_{injected}$ = 250 µL, Q = 1.5 mL/min), b) influence of the flow rate ($V_{injected}$ = 500 µL, c = 5 g/L), c) influence of the injected volume (Q = 1.5 mL/min, c = 5 g/L), d) influence of the injected volume vs. concentration (Q = 1.5 mL/min, $m_{injected}$ = 2.5 mg).

For effective separation of free chitosan, the characteristic shoulder corresponding to the chitosan must be clearly visible on the chromatograms. Since the flow rate did not significantly impact the peak resolution, a flow rate of 1.5 mL/min was preferred to avoid long elution times. Lower injected volumes and polymer concentrations resulted in better peak resolution. In order to maximize the recovered mass of free chitosan, a comparison was made between the combined influence of these two parameters while keeping the injected mass constant. It was found that a low concentration was preferable over a low injected volume for achieving better separation. The optimized experimental parameters were as follows: polymer concentration = 5 g/L, injected volume = 500 µL, flow rate = 1.5 mL/min. This results

in an injected mass of 2.5 mg per analysis, each analysis lasting 90 minutes. The different fractions are collected every 3.5 min from 55 min to 75 min of elution.

After collecting the fractions, they were dialyzed for 48 hours against water using float-a-lyzer devices with MW cut-off of 500 Da in order to remove the salts from the elution buffer. After freeze drying, the different fractions were resolubilized in acetate buffer and analyzed by analytical SEC (Figure S16).

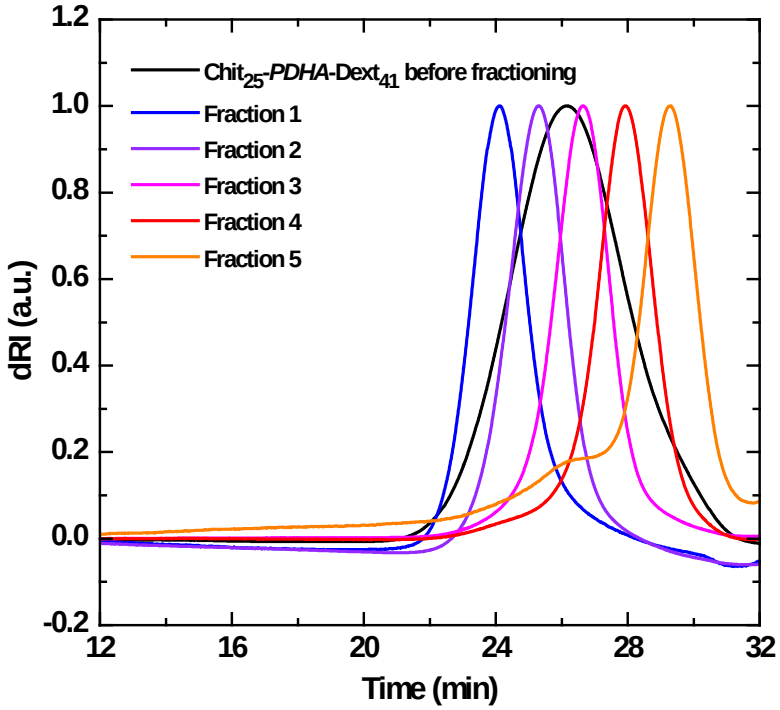

Figure S18. Chromatograms of the different fractions of $Chit_{25}$-*PDHA*-$Dext_{41}$ collected by semi-preparative SEC and analyzed by analytical SEC in 0.2 M acetate buffer AcOH/0.15 M AcONa pH 4.5. Each chromatogram is scaled against its own magnitude.

The fraction 5 contains mostly free chitosan, with some copolymers present as indicated by the shoulder on the left of the peak. As a precaution, fractions 4 and 5 were excluded to ensure the removal of the majority of free chitosan. Although highly effective, semi-preparative SEC fractionation is nevertheless a time-consuming method with low yields and requiring an additional dialysis step. To obtain 100 mg of purified copolymers, at least 160 mg should be injected, requiring approximately 4 days of fractionation under the described conditions.

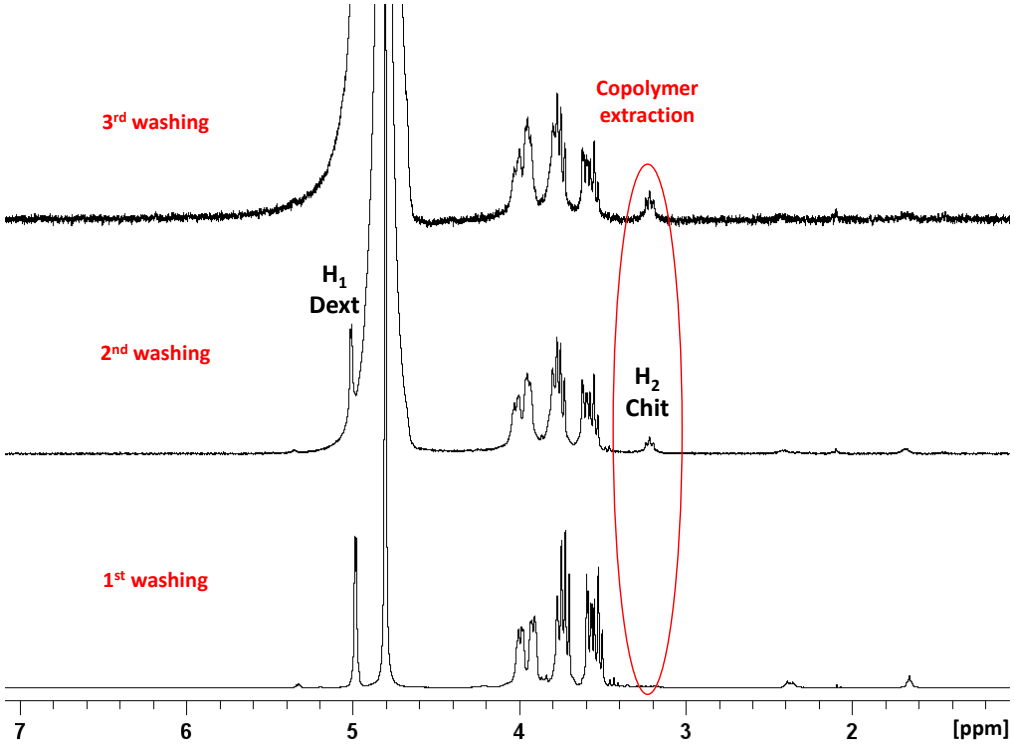

Figure S19. Purification of $Chit_{25}$-*ADH*-$Dext_{41}$ to remove excess $Dext_{41}$-ADH by precipitation in basic pH conditions followed by repetitive centrifugation and washings with D_2O. ^1H NMR analysis of supernatants indicated significant copolymer extraction starting from the second washing.

Table S6. Masses recovered from the pellet and the supernatant after centrifugation of $Chit_{25}$-*PDHA*-$Dext_{41}$ copolymer solutions adjusted at various pHs.

	pH 6.5	**pH 6.7**	**pH 7.0**
m_{pellet} (mg)	2.8	4.4	6.9
$m_{supernatant}$ (mg)	22.4	20.3	17.2
pellet (wt. %)	11	18	29

S8. Block copolysaccharides library

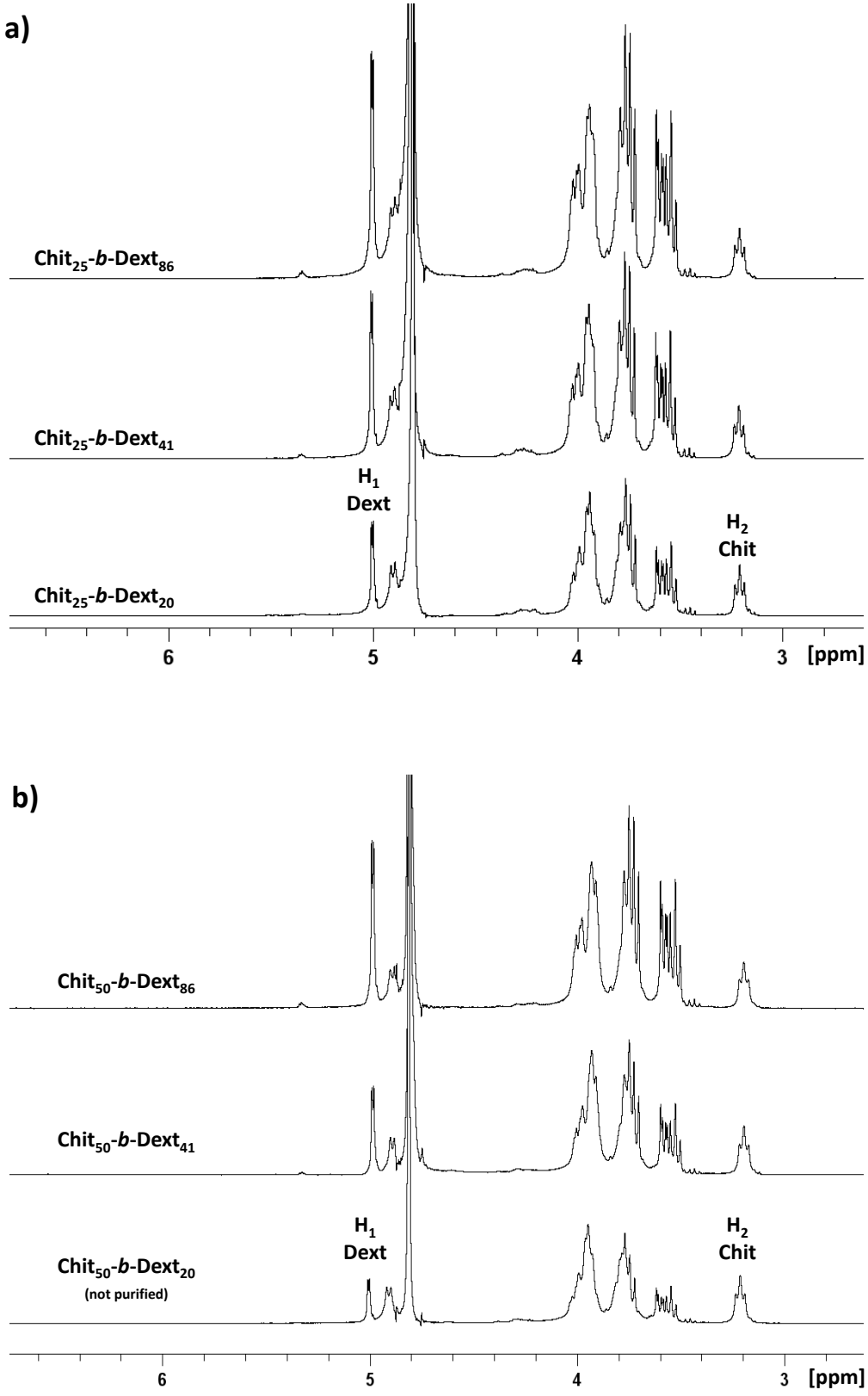

Figure S20. ^{1}H-NMR spectra of the block copolysaccharides after purification by selective precipitation of free chitosan at pH 6.5. a) Chit$_{25}$-*b*-Dext$_{20}$, Chit$_{25}$-*b*-Dext$_{41}$ and Chit$_{25}$-*b*-Dext$_{86}$ and b) Chit$_{50}$-*b*-Dext$_{20}$ (not purified), Chit$_{50}$-*b*-Dext$_{41}$ and Chit$_{50}$-*b*-Dext$_{86}$.

References

(1) Hirai, A.; Odani, H.; Nakajima, A. Determination of Degree of Deacetylation of Chitosan by 1H NMR Spectroscopy. *Polymer Bulletin* **1991**, *26* (1), 87–94. https://doi.org/10.1007/BF00299352.

(2) Gagnaire, D.; Vignon, M. Étude Par 13C NMR et 1H NMR Du Dextrane et de Ses Dérivés Acétylés et Benzylés. *Die Makromolekulare Chemie* **1977**, *178* (8), 2321–2333. https://doi.org/10.1002/macp.1977.021780819.

(3) Chapelle, C.; David, G.; Caillol, S.; Negrell, C.; Durand, G.; Desroches le Foll, M.; Trombotto, S. Water-Soluble 2,5-Anhydro- D -Mannofuranose Chain End Chitosan Oligomers of a Very Low Molecular Weight: Synthesis and Characterization. *Biomacromolecules* **2019**, *20* (12), 4353–4360. https://doi.org/10.1021/acs.biomac.9b01003.

(4) Mo, I. V.; Dalheim, M. Ø.; Aachmann, F. L.; Schatz, C.; Christensen, B. E. 2,5-Anhydro-d-Mannose End-Functionalized Chitin Oligomers Activated by Dioxyamines or Dihydrazides as Precursors of Diblock Oligosaccharides. *Biomacromolecules* **2020**, *21* (7), 2884–2895. https://doi.org/10.1021/acs.biomac.0c00620.